To appear in Physics Uspekhi

High – Temperature Superconductivity in Iron Based Layered Compounds

M. V. Sadovskii
Institute for Electrophysics, Russian Academy of Sciences, Ural Branch, 620016 Ekaterinburg, Russia

We present a review of basic experimental facts on the new class of high – temperature superconductors — iron based layered compounds like REOFeAs (RE=La,Ce,Nd,Pr,Sm...), AFe_2As_2 (A=Ba,Sr...), AFeAs (A=Li,...) and FeSe(Te). We discuss electronic structure, including the role of correlations, spectrum and role of collective excitations (phonons, spin waves), as well as the main models, describing possible types of magnetic ordering and Cooper pairing in these compounds [1].

PACS numbers: 74.25.Jb, 74.20.Rp, 74.25.Dw, 74.25.Ha, 74.20.-z, 74.20.Fg, 74.20.Mn, 74.62.-c, 74.70.-b

Contents

[1] *Extended version of the talk given on the 90th anniversary celebration of Physics Uspekhi, P.N. Lebedev Physical Institute, Moscow, November 19, 2008.*

INTRODUCTION

The discovery more than 20 years ago of high – temperature superconductivity (HTSC) in copper oxides [1] attracted much interest and has lead to publication of thousands of experimental and theoretical papers. During these years a number of reviews were published in Physics Uspekhi, which were devoted to different aspects of superconductivity in cuprates and perspectives of further progress in the growth of the critical temperature of superconducting transition T_c, which appeared both immediately after this discovery [2, 3, 4] and much later [5, 6, 7, 8, 9, 10]. Physics of HTSC and of a number of new and unusual superconductors was discussed in a number of individual and collective monographs [11, 12, 13, 14].

Unfortunately, despite these unprecedented efforts of researchers all over the world, the physical nature of high – temperature superconductivity in cuprates is still not completely understood. Basic difficulties here are attributed to the significant role of electronic correlations – in the opinion of the majority of authors cuprates are strongly correlated systems, which lead to anomalies of the normal state (inapplicability of Fermi – liquid theory) and the wide spectrum of possible explanations of microscopic mechanism of superconductivity – from relatively traditional [6, 9] to more or less exotic [12].

In this respect, the discovery in the early 2008 of a new class of high – temperature superconductors, i.e. layered compounds based on iron [15], has attracted a tremendous interest. This discovery has broken cuprate "monopoly" in the physics of HTSC compounds and revived hopes both on further progress in this field related to the synthesis of new perspective high – temperature superconductors, as well as on more deep theoretical understanding of mechanisms of HTSC. Naturally, the direct comparison of superconductivity in cuprates and new iron based superconductors promises the identification of common anomalies of these systems, which are relevant for high values of T_c, as well as important differences not directly related to the phenomenon of high – temperature superconductivity and, in fact, complicating its theoretical understanding.

The aim of the present review is a short introduction into the physics of new iron based layered superconductors and comparison of their properties with well established facts concerning HTSC in copper oxides. Progress in this field is rather spectacular and rapid, so that this review is in no sense exhaustive [1]. However, the author hopes that it may be a kind of elementary introduction into this new field of research and may help a more deep studies of original papers.

[1] It is sufficient to say that during the first six months of the studies of new superconductors about 600 original papers (preprints) were published. Obviously, in this review it is even not possible just to cite all these works and our choice of citations is rather subjective. The author pays his excuses in advance to those authors of important papers, which remained outside our reference list, as this is attributed to obvious limitations of size and author's own ignorance.

Anomalies of high–temperature superconductivity in copper oxides

At present dozens of HTSC compounds based on copper oxides are known to have temperature of superconducting transition T_c exceeding 24K [16]. In Table I we present critical temperatures for number of most "popular" cuprates.

Table I. Temperatures of superconducting transition in copper oxides[2].

Compound	T_c(K)
$HgBa_2Ca_2Cu_3O_{8+\delta}$	134
$Tl_2Ca_2Ba_2Cu_3O_{10}$	127
$YBa_2Cu_3O_7$	92
$Bi_2Sr_2CaCu_2O_8$	89
$La_{1.83}Sr_{0.17}CuO_4$	37
$Nd_{1.85}Ce_{0.15}CuO_4$	24

More than 20 years of experience has lead to rather deep understanding of the nature of superconductivity in these systems. It is clear for example, that HTSC in cuprates is not connected with some "essentially new" physics, which is different in comparison with other superconductors, superfluid Fermi – liquids like He^3, nucleons in atomic nuclei or nuclear matter in neutron stars, dilute Fermi – gases with Cooper pairing actively studied at present, or even hypothetical "color" superconductivity of quarks.

In this respect let us list

What do we definitely know about cuprates:

- *The nature of superconductivity in cuprates* $\rightleftharpoons$ *Cooper pairing.*

  1. This pairing is anisotropic and of d – type, so that the energy gap acquires zeroes at the Fermi surface: $\Delta \cos 2\phi$, where ϕ is the polar angle, determining momentum direction in the two – dimensional Brillouin zone.
  2. The size of Cooper pairs (coherence length at zero temperature $T = 0$) is relatively small: $\xi_0 \sim 5 - 10a$, where a is the lattice constant in CuO_2 plane.

- *There exists a relatively well defined (at least in the part of the Brillouin zone) Fermi surface, in this sense these systems are metals.*

- *However, appropriate stoichiometric compounds are antiferromagnetic insulators — superconductivity is realized close to the Mott metal – insulator phase transition (controlled by composition) induced by strong electronic correlations.*

- *The strong anisotropy of all electronic properties is observed — conductivity (and superconductivity) is realized mainly within* CuO_2 *layers (quasi two–dimensionality!).*

At the same time, many things are still not understood. Accordingly, we may list

What do we not really know about cuprates:

- *Mechanism of Cooper pairing (a "glue" leading to formation of Cooper pairs).*

  Possible variants:

  1. Electron – phonon mechanism.

[2] Under pressure T_c of $HgBa_2Ca_2Cu_3O_{8+\delta}$ reaches $\sim$ 150K.

2. Spin fluctuations.
3. Exchange – RVB, $SO(5)$, or something more "exotic".

The difficulties of choice here are mainly due to the unclear

- *Nature of the normal state.*

1. Is Fermi – liquid theory (Landau) valid here?
2. Or some more complicated scenario is realized, like "marginal" or "bad" Fermi – liquid?
3. Possible also is some variant of Luttinger liquid, essentially different from Fermi – liquid.
4. Still mysterious is the nature of the pseudogap state.
5. Not completely clear is the role of internal disorder and local inhomogeneities.

Of course, we observe continuous, though slow, progress. For example, most researchers are now leaning towards spin – fluctuation (non phonon) mechanism of pairing. Pseudogap state is most likely connected with fluctuations of some competing (with superconductivity) order parameter (antiferromagnetic or charged) [17, 18]. Fermi – liquid description is apparently applicable in the most part of the Brillouin zone, where Fermi surface remains not "destroyed" by pseudogap fluctuations etc. However, the consensus in HTSC community is still absent, which is obviously related to the complicated nature of these systems, controlled beforehand by strong electronic correlations, which control this nature and complicate theoretical understanding. Just because of that, the discovery of a new class of HTSC compounds promises definite hopes as new possibilities of HTSC studies in completely different systems appear, where some of these difficulties may be just absent.

Other superconductors with unusual properties

Obviously, during all the years since the discovery of HTSC in cuprates active efforts continued in the search of new compounds with potentially high temperatures of superconducting transition. A number of systems obtained during this search are listed in Table II.

Table II. Temperatures of superconducting transition in some "unusual" superconductors.

Compound	T_c(K)
MgB_2	39
$RbCs_2C_{60}$	33
K_3C_{60}	19
Sr_2RuO_4	1.5

Despite the obvious interest from the point of view of physics and unusual properties of some of these systems there were no significant progress on this way. This was mainly due to the fact that all the systems listed in Table II are, in some sense, "exceptional" – none is a representative of a wide class of compounds with a possibility of a change of system properties (parameters) in a wide range, as in cuprates. All these systems were studied in detail, and summaries of these studies can be found in the relevant reviews [19, 20, 21, 22, 23]. In fact, all these studies have added very little to our understanding of the cuprates. Up to now there was kind of "cuprate monopoly" in the physics of "real" HTSC materials with wide perspectives of further studies and search of compounds with even higher values of T_c and practical applications[3].

[3] Surely, when we speak about practical applications we should not underestimate the perspectives of MgB_2 compound.

BASIC EXPERIMENTAL FACTS ON NEW SUPERCONDUCTORS

Electrical properties and superconductivity

$REOFeAs$ ($RE = La, Ce, Pr, Nd, Sm, ...$) system

Discovery of superconductivity with $T_c = 26$K in $LaO_{1-x}F_xFeAs$ ($x = 0.05 - 0.12$) [15] was preceded by the studies of electrical properties of a number of oxypnictides like $LaOMPn$ ($M = Mn, Fe, Co, Ni$ and $Pn = P, As$) highlighted by discovery of superconductivity in $LaOFeP$ with $T_c \sim 5$K [24] $LaONiP$ $T_c \sim 3$K [25], which has not attracted much attention from HTSC community. This situation has changed sharply after Ref. [15] has appeared and shortly afterwards a lot of papers followed (see e.g. [26, 27, 28, 29, 30, 31, 32, 33, 34, 35]), where this discovery was confirmed and substitution of lanthanum by a number of other rare – earths, according to a simple chemical formula $(RE)^{+3}O^{-2}Fe^{+2}As^{-3}$, has lead to more than doubling of T_c up to the values of order of 55K in systems based upon $NdOFeAs$ and $SmOFeAs$, with electron doping via addition of fluorine or creating oxygen deficit, or hole doping achieved by partial substitution of the rare – earth (e.g. La by Sr) [36]. Note also Ref. [37], where the record values of $T_c \sim 55$K were achieved by partial substitution of Gd in $GdOFeAs$ by Th, which, according to the authors, also corresponds to electron doping. In these early works different measurements of electrical and thermodynamic properties were performed on polycrystalline samples.

In Fig. 1 (a), taken from Ref. [33], we show typical temperature dependences of electric resistivity in different $REOFeAs$ compounds. It can be seen that for most of these compounds T_c is within the interval 40-50K, while $LaOFeAs$ system drops out with its significantly lower transition temperature ~ 25K. In this respect we can mention Ref. [34] in which a synthesis of this system under high pressure was reported, producing samples with T_c (onset of superconducting transition) of the order of 41K. In Ref. [38] analogous increase of T_c in this system was achieved under external pressure ~ 4GPa. Probably this last result is characteristic only for La system, as further increase of pressure leads to the drop of T_c, while in other systems (e.g. Ce based) T_c lowers with the increase of external pressure from the very beginning (see. e.g. Ref. [39, 40]).

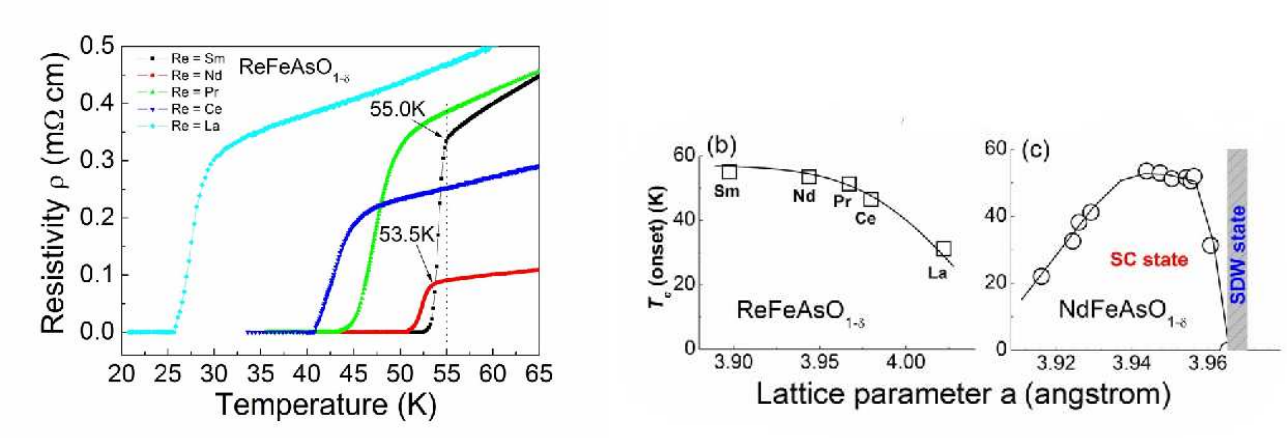

FIG. 1: (a) resistivity behavior in REOFeAs (RE=La,Ce,Pr,Nd, Sm) close to superconducting transition, (b,c) T_c dependence on the value of the lattice constant [33].

In many papers the growth of T_c, induced by La substitution by other rare – earths (with smaller ion radius) is often attributed to "chemical" pressure, which is illustrated e.g. by qualitative dependence of T_c on lattice spacing, shown in Fig. 1 (b) [33]. At the same time, Fig. 1 (c) taken from the same work shows that lattice compression leads to the growth of T_c only up to a certain limit, and after that T_c drops (compare it with results of high pressure experiments mentioned above).

In more wide temperature interval typical temperature behavior of resistivity is illustrated by the data for $CeO_{1-x}F_xFeAs$ shown in Fig. 2, taken from Ref. [30]. It can be seen that the prototype system $CeOFeAs$ is characterized by *metallic* behavior of resistivity up to the lowest temperatures achieved, with characteristic anomaly in the vicinity of $T \sim 145$K and sharp drop of resistivity at lower temperatures. Metallic nature of prototype $REOFeAs$ systems contrasts with insulating nature of stoichiometric cuprates. After doping, e.g. by fluorine, the value of resistivity drops, its anomaly becomes less visible and disappears at higher dopings, where superconductivity

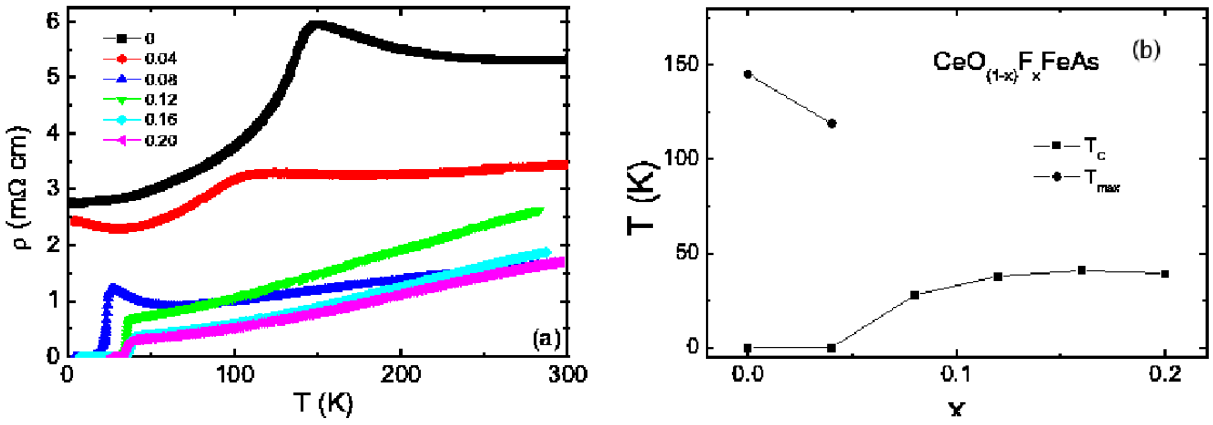

FIG. 2: (a) temperature dependence of resistivity in $CeO_{1-x}F_xFeAs$ for different compositions x, shown on the graph, (b) phase diagram showing superconducting region and concentration dependence of high – temperature anomaly T_{max} of resistivity, associated with SDW transition [30].

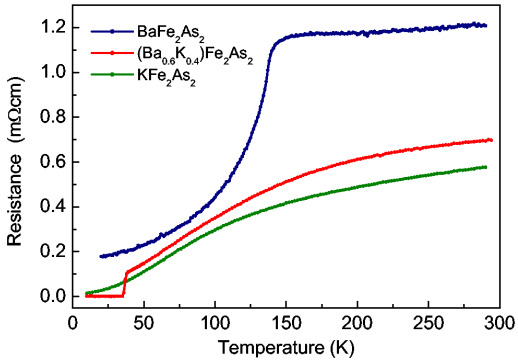

FIG. 3: Temperature dependence of resistivity in $Ba_{1-x}K_xFe_2As_2$ for different compositions x, shown on the graph [45].

appears. The highest value of $T_c = 41$K is achieved for $x = 0.16$, and the resulting F concentration phase diagram is shown in Fig. 2. High temperature anomaly of resistivity in prototype and slightly doped system in most of the works is attributed to structural phase transition and (or) accompanying spin density wave (SDW) transition, while its degradation under doping is usually connected with the breaking of "nesting" of the Fermi surfaces (cf. below). This behavior of resistivity is rather typical and is observed in all $REOFeAs$ systems (cf. e.g. Ref. [32]), which are for shortness called now 1111 – systems.

In fact, to the same class belongs the recently synthesized compound Sr(Ca)FFeAs [41, 42]. Here the typical SDW anomaly of resistivity is observed in the vicinity of 175 K. Further doping of this system with Co has lead to the appearance of superconductivity with T_c ∼5 K [43], while in $Sr_{1-x}La_x$FFeAs superconducting transition with T_c=36 K [44] was obtained.

AFe_2As_2 $(A = Ba, Sr, ...)$ system

More simple (structurally and chemically) class of iron based superconductors was discovered in Ref. [45], by the synthesis of $Ba_{1-x}K_xFe_2As_2$ compound, superconductivity with $T_c = 38$K was observed for $x = 0.4$. The relevant data on the temperature dependence of resistivity are shown in Fig. 3 [45].

In the prototype compound $BaFe_2As_2$ temperature dependence of resistivity demonstrates typically metallic behavior with characteristic anomaly in the vicinity of $T \sim 140$K, which is connected to a spin density wave (SDW) and structural phase transition (cf. below). According to a simple chemical formula $Ba^{+2}(Fe^{+2})_2(As^{-3})_2$, the partial

substitution of Ba^{+2} by K^{+1} leads to hole doping, which suppresses SDW transition and leads to superconductivity in some concentration interval. Obviously, these results are quite similar to quoted above for $REOFeAs$ systems (1111).

In Ref. [48] a similar behavior was obtained in $Sr_{1-x}K_xFe_2As_2$ with maximal $T_c \sim 38$K, while in Ref. [51] the systems like AFe_2As_2 with $A = K, Ca, K/Sr, Ca/Sr$ were studied, and electron doping by Sr of compounds with $A = K \quad A = Cs$ produced values of $T_c \sim 37$K followed by SDW transition. This new class of Fe based HTSC is sometimes denoted for shortness as 122 systems.

Note also an interesting paper [49], where superconductivity with T_c up to 29K was obtained in prototype (undoped) compounds $BaFe_2As_2$ and $SrFe_2As_2$ under external pressure, but only in a limited interval of pressures. Superconductivity also appears under electron doping of these systems by Co [50].

$AFeAs$ ($A = Li, ...$) system

One more type of Fe based superconductors is represented by $Li_{1-x}FeAs$ (111) system, where superconductivity appears at $T_c \sim 18$K [52, 53]. Up to now there are few works on this system, however, it is clear that it is quite similar to 1111 and 122 systems and is rather promising in a sense of comparison of its properties with those of other systems, discussed above.

$FeSe(Te)$ system

Finally, rather unexpectedly, superconductivity was discovered in very "simple" $\alpha - FeSe_x$ ($x < 1$) system [54] with $T_c = 8$K, reaching 27K under pressure of 1.48GPa [55]. Next the system $Fe(Se_{1-x}Te_x)_{0.82}$ was also studied, and the maximum value of $T_c = 14$K was achieved for $0.3 < x < 1$ [56]. Here there are still very few detailed studies, though it is quite clear that electronic structure these systems are again similar to those discussed above, so that in the nearest future we can expect a lot of papers devoted to the comprehensive studies of their electronic properties.

Search for new systems

Naturally, at present an active search of other similar systems is underway with the hope to obtain even higher values of T_c. Up to now, outside the domain of FeAs based systems, successes are rather modest. We shall mention only few works, were new superconductors were synthesized.

We have already mentioned compounds like $LaOFeP$ with $T_c \sim 5$K [24] and $LaONiP$ with $T_c \sim 3$K [25], which are representatives of the same class of superconducting oxypnictides (1111), as the whole series of $REOFeAs$. Superconductivity with $T_c \sim 4$K was discovered in $LaO_{1-\delta}NiBi$ compound [57], while in $GdONiBi$ and $Gd_{0.9}Sr_{0.1}ONiBi$ the value of $T_c \sim 0.7$K was obtained in Ref. [58]. Transition temperature $T_c \sim 2.75$K was obtained in $LaO_{1-x}F_xNiAs$ [59].

In the class of 122 systems the value of $T_c \sim 0.7$K was obtained in $BaNi_2As_2$ [60].

An interesting new system $La_3Ni_4P_4O_2$ with different crystal structure demonstrated superconductivity at $T_c \sim 2.2$K [61]. In this reference a number of promising systems of the same type were also discussed.

Surely, all these results are not very exciting. However, there is rather large number of systems somehow similar to already known FeAs compounds and where we can also expect. A wide set of promising compounds was discussed in Ref. [62].

Crystal structure and anisotropy

Crystal structure of $BaFe_2As_2$ and LaOFeAs compounds and their analogs corresponds to tetragonal symmetry and space groups $I4/mmm$ and $P4/nmm$. Both compounds are formed by the layers of $(FeAs)^-$ with covalent bonding, interlaced by the layers of $Ba^{2+}_{0.5}$ or $(LaO)^+$, while interlayer bonding is ionic. Ions of Fe^{2+} are surrounded by four ions of As, which form tetrahedra. The general view of crystal structures of LaOFeAs and $BaFe_2As_2$ is shown in Fig. 4. Layered (quasi two – dimensional) nature of these compounds is similar to that of HTSC cuprates. At 140K $BaFe_2As_2$ undergoes the structural phase transition from tetragonal ($I4/mmm$) to orthorhombic ($Fmmm$)

structure [46]. Analogous transition takes place also in LaOFeAs at 150 K: $P4/nmm$ (tetragonal) $\rightarrow$ $Cmma$ (orthorhombic) [47]. Experimental atomic positions in $BaFe_2As_2$ are: Ba (0, 0, 0), Fe (0.5, 0, 0.25), As (0, 0, z). For LaOFeAs these are: La(0.25, 0.25, z), Fe (0.75, 0.25, 0.5), As (0.25, 0.25, z), O (0.75, 0.25, 0). The rest of crystallographic data for both compounds are given in Table III. It is seen that in $BaFe_2As_2$ the Fe-As distance is smaller than in LaOFeAs. Thus in $BaFe_2As_2$ we can expect stronger Fe-d-As-p hybridization in comparison with LaOFeAs and, correspondingly, the larger d-band width for Fe. Similarly, the distance between adjacent atoms of Fe within the layers of FeAs in $BaFe_2As_2$ is also significantly smaller than in LaOFeAs (and related compounds). After the phase transition of $BaFe_2As_2$ into orthorhombic structure the four (initially equal) Fe-Fe distances are separated into two pairs of bonds with the widths of 2.808 Å and 2.877 Å. Moreover, two As-Fe-As angles are significantly different in LaOFeAs system (113.6° and 107.5°) and very close ($\sim 109°$) in $BaFe_2As_2$. Such differences in the nearest neighborhood of Fe ions should lead to appropriate changes in their electronic structure.

Table III. Structural data for $BaFe_2As_2$ and LaOFeAs.

Parameters	$BaFe_2As_2$	LaOFeAs
Group	I4/mmm	P4/nmm
a, Å	3.9090(1)	4.03533(4)
c, Å	13.2122(4)	8.74090(9)
z_{La}	-	0.14154(5)
z_{As}	0.3538(1)	0.6512(2)
Reference	[45]	[15]
Ba-As, Å	3.372(1)×8	-
La-As, Å	-	3.380×4
Fe-As, Å	2.388(1)×4	2.412×4
Fe-Fe, Å	2.764(1)×4	2.853×4
As-Fe-As	109.9(1)°	113.6°
	109.3(1)°	107.5°

Doping of prototype REOFeAs compounds by fluorine (or by creation of oxygen deficit) or $BaFe_2As_2$ by substitution of Ba(Sr) by K etc., leads to the suppression of transition from tetragonal to orthorhombic structure and appearance of superconductivity in tetragonal phase.

Recently, the crystal structure of LiFeAs compound was also refined [53]. LiFeAs forms tetragonal structure with space group $P4/nmm$ and lattice parameters $a = 3.7914(7)$ Å, $c = 6.364(2)$ Å. Experimentally determined atomic positions are: Fe(2b) (0.75, 0.25, 0.5), Li(2c) (0.25, 0.25, z_{Li}), As(2c) (0.25, 0.25, z_{As}), z_{As}=0.26351, z_{Li}=0.845915 [53]. Crystal structure of LiFeAs is shown in Fig. 5 (a) and is again characterized by its layered nature, which suggests quasi two – dimensional electronic properties and is clearly analogous to the structure of LaOFeAs [15] and $BaFe_2As_2$ [46]. Most important Fe-Fe and Fe-As distances are 2.68 and 2.42 Å correspondingly. At present this structure is most spatially compact among similar compounds. As-Fe-As angles in LiFeAs has the values of $\sim 103.1°$ and $\sim 112.7°$, which also can lead to some fine differences of electronic structure in comparison with LaOFeAs and $BaFe_2As_2$.

Crystal structure of α-FeSe is especially simple – it forms the layered tetragonal phase (like PbO) with square sublattice of Fe and space group $P4/nmm$. The crystal of α-FeSe consists of layers of $FeSe_4$ edge-sharing tetrahedra as shown in Fig. 5 (b). Experimentally determined [54] lattice constants are: $a = 3.7693(1)$ Å, $c = 5.4861(2)$ Å for $FeSe_{0.82}$ and $a = 3.7676(2)$ Å, $c = 5.4847(1)$ Å for $FeSe_{0.88}$. Analogy with oxypnictides like REOFeAs and systems like $BaFe_2As_2$ is obvious. At $T \sim 105$K this system undergoes the phase transition from tetragonal to triclinic structure (group P-1) [54].

Up to now only very small single crystal of 1111 compounds were successfully synthesized ($\sim 100 \times 100\ \mu m^2$) (cf. e.g. Refs. [63, 64]). Situation with 122 systems is much better, here almost immediately the crystals of millimeter sizes were obtained (see Fig. 6) [65]. Thus, most of the measurements in the following were made on single crystals of this system (though for 1111 system a number of interesting studies on single crystals were also performed). Recently rather small single crystals ($\sim 200 \times 200\ \mu m^2$) of $\alpha - FeSe$ with $T_c \sim 10$K [66] were also obtained, but detailed physical measurements on this system are still to be done.

Typical results of measurements on single crystals of 1111 [64] and 122 [65] systems are shown in Fig. 6. In particular, the anisotropy of the upper critical field H_{c2} corresponds quasi two – dimensional nature of electronic subsystem of these superconductors, which is already evident from their crystal structure. At the same time, we can see that this anisotropy of critical fields is not too large.

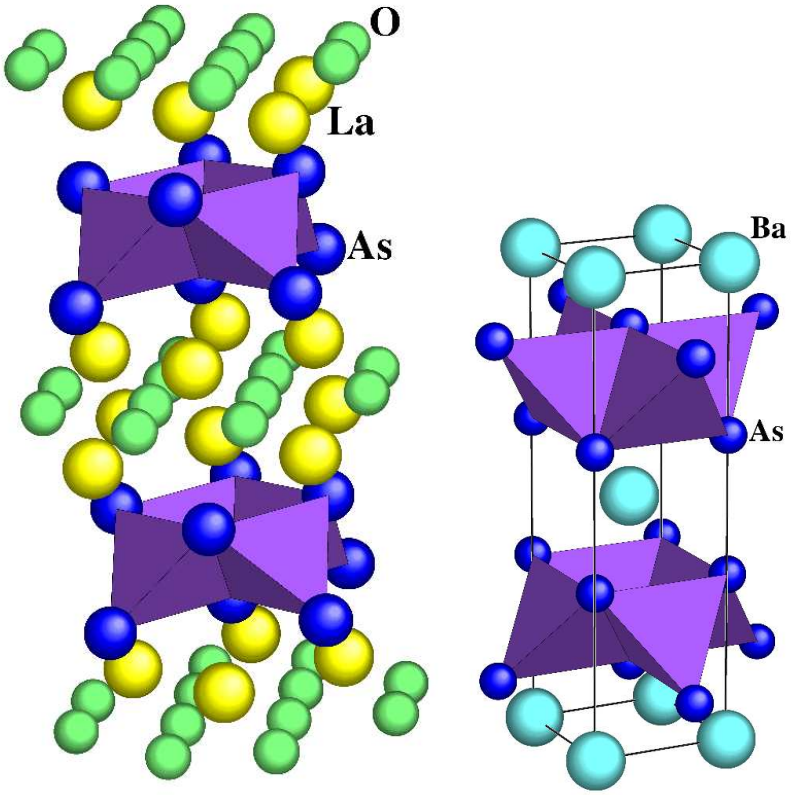

FIG. 4: Crystal structure of LaOFeAs (left) and $BaFe_2As_2$ (right). FeAs tetrahedra form two - dimensional layers, surrounded by the layers of LaO or Ba. Fe ions inside tetrahedra form square lattice.

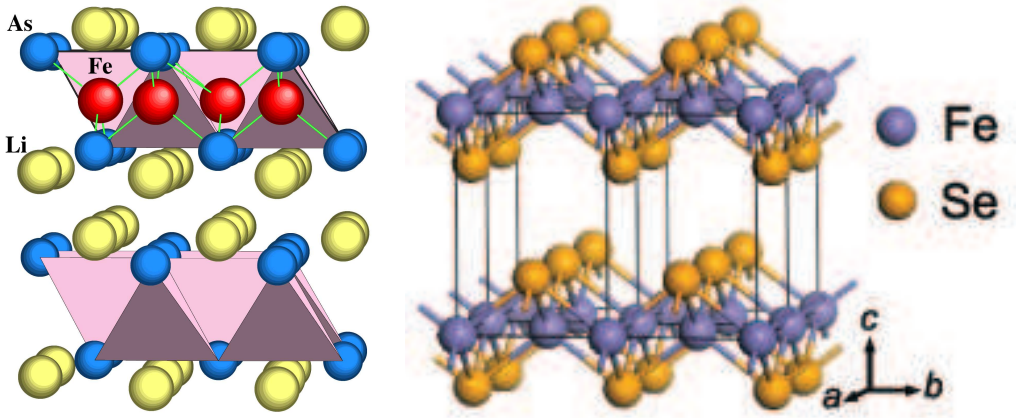

FIG. 5: Crystal structure of LiFeAs (left). FeAs tetrahedra form two – dimensional layers separated by layers of Li ions. At right – crystal structure of α-FeSe.

In Fig. 7 from Ref. [67] we show temperature dependence of resistivity ρ_{ab} in ab plane and of transverse resistivity ρ_c in orthogonal direction for the single crystal of prototype (undoped) $BaFe_2As_2$ system [67]. It can be seen that anisotropy of resistivity exceeds 10^2, which confirms the quasi two – dimensional nature of electronic properties of this system. This anisotropy is significantly larger than the value which can be expected from the simple estimates[4],

[4] Anisotropy of H_{c2} is usually of the order of square root of the anisotropy of resistivity.

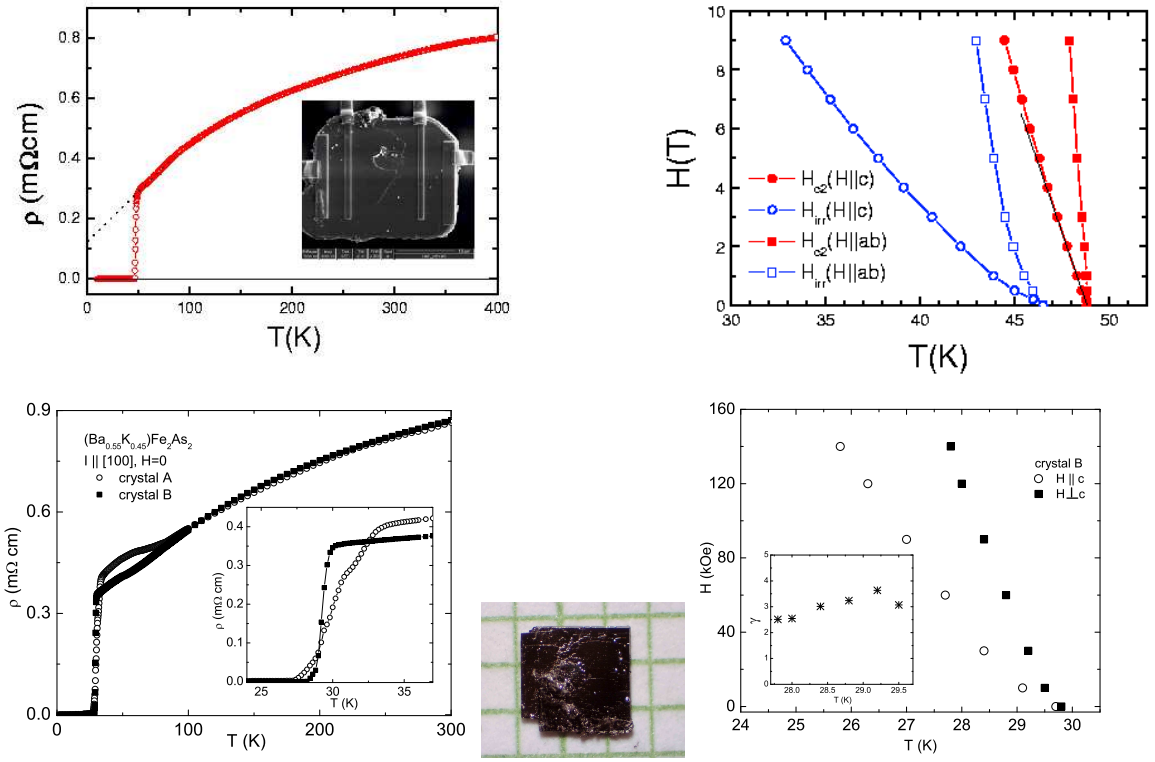

FIG. 6: (a) superconducting transition and anisotropic behavior of the upper critical field H_{c2} (and irreversibility field H_{irr}) (b) in the single crystal of $NdO_{0.82}F_{0.18}FeAs$ [64], (c) superconducting transition and anisotropic behavior of the upper critical field H_{c2} (d) in the single crystals of $Ba_{1-x}K_xFeAs$ [65], where at the insert we also show small temperature dependence of anisotropy of H_{c2}. In the photo – typical single crystal of $Ba_{1-x}K_xFe_2As_2$.

based on the anisotropy of H_{c2}. However, we must stress that data on the anisotropy of resistivity of superconducting samples in Refs. [65, 67] is just absent. In the data shown in Fig. 7 we can also clearly see an anomaly in temperature dependence of resistivity at $T_s = 138$K, connected with antiferromagnetic (SDW) transition.

The question of anisotropy of electronic properties has sharpened after in Ref. [68] the measurements of H_{c2} in single crystals of $Ba_{1-x}K_xFe_2As_2$ were performed in much wider temperature interval than in [65], up to the field values of the order of ~ 60T. According to Ref. [68] anisotropy of H_{c2} is observed only in relatively narrow temperature interval close to T_c, changing to almost isotropic behavior as temperature lowers.

Magnetic structure and phase diagram

As we have already mentioned, as temperature lowers prototype (undoped) 1111 and 122 compounds undergo structural transition accompanied by simultaneous or later antiferromagnetic transition (probably of SDW type). Direct confirmation of this picture was obtained in neutron scattering experiments. First results for $LaOFeAs$ system were given in Ref. [69]. It was discovered that the structural transition in this compound (according to Ref. [69] from orthorhombic $P4/nmm$ into monoclinic $P112/n$ structure, which differs from the results of other authors [47]) takes place at $T \sim 150$K (where anomaly in temperature dependence of resistivity is observed), and afterwards at $T \sim 134$K antiferromagnetic ordering appears.

In Fig. 8 (a) we show antiferromagnetic structure obtained in these experiments, as well as temperature dependence of the square of magnetic moment at Fe site. The value of this moment is not larger than 0.36(5) μ_B. We see that spin ordering in the ab plane takes the form of characteristic chains of ferromagnetically oriented spins with opposite spin orientations in neighboring chains (stripes). Along c axis there is typical period doubling.

In Fig. 8 (b) we compare the magnetic structures in CuO_2 plane of cuprates and in $FeAs$ plane of new FeAs based

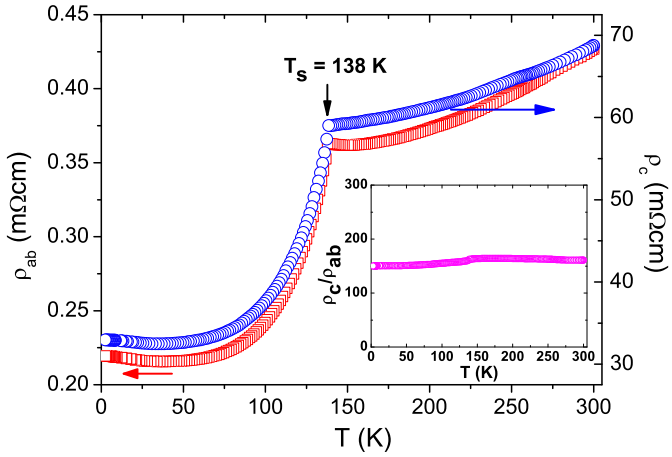

FIG. 7: Temperature dependence of resistivity ρ_{ab} in the ab plane and transverse resistivity ρ_c in orthogonal direction in the single crystal of $BaFe_2As_2$ [67]. At the insert – temperature dependence of resistivity anisotropy.

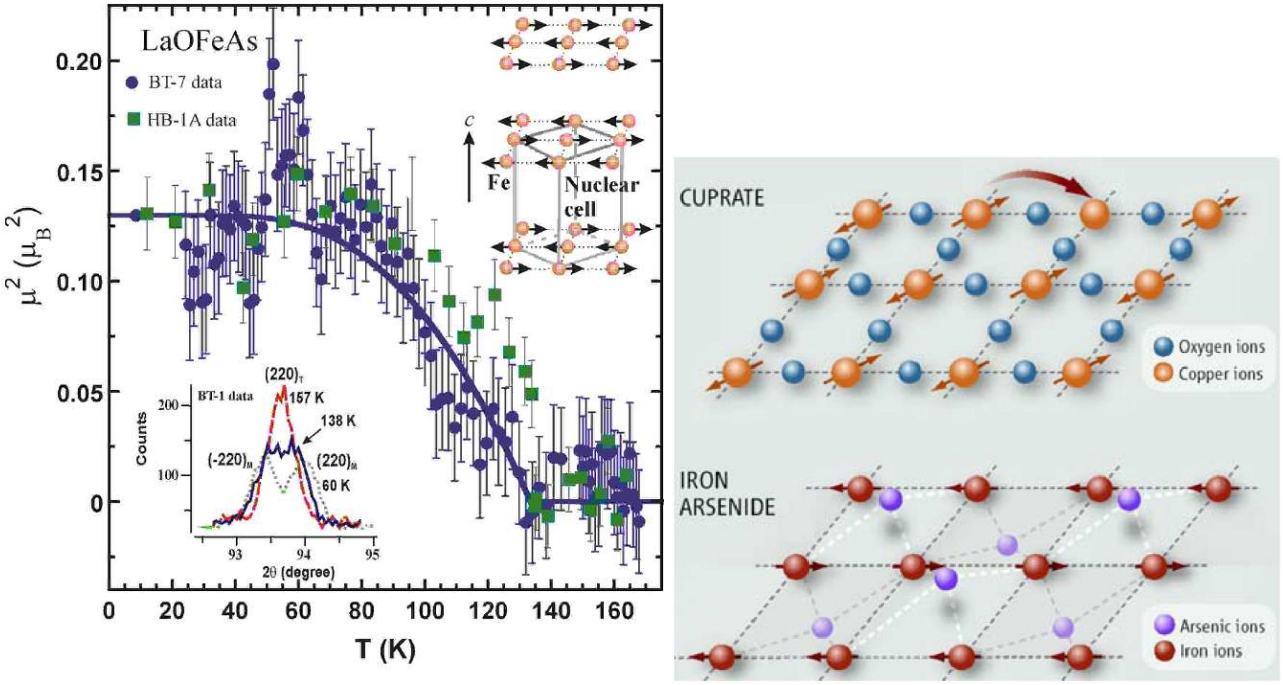

FIG. 8: (a) temperature dependence of the square of magnetic moment on Fe in LaOFeAs obtained by neutron scattering (data from two spectrometers denoted as BT-7 and HB-1A) [69]. At the insert in the upper right corner – the experimentally determined antiferromagnetic structure in $\sqrt{2}a \times \sqrt{2}b \times 2c$ lattice cell. Distortion of the nuclear scattering peak shown at the insert in the lower left corner shows that structural transition precedes magnetic transition. (b) comparison of antiferromagnetic ordering in CuO_2 plane of cuprates and in $FeAs$ plane of new superconductors.

superconductors. Both analogy and significant difference can be clearly seen. Both structural and antiferromagnetic transitions in $FeAs$ planes are suppressed by doping, similarly to situation in cuprates. At the same time it should be stressed that antiferromagnetic phase of cuprates is an insulator, while in $FeAs$ superconductors it remains metallic, as is clearly seen from the data on resistivity quoted above.

Phase diagram of new superconductors (with changing concentration of doping element) is also significantly different from that of cuprates. In Fig. 9 we show this phase diagram for $LaO_{1-x}F_xFeAs$ system, obtained in Ref. [70] from μSR experiments. It can be seen that temperatures of structural and magnetic transitions are clearly separated, while superconductivity region does not overlap with antiferromagnetic region.

Analogous phase diagram for $CeO_{1-x}F_xFeAs$, obtained in Ref. [71] from neutron scattering data is shown in Fig.

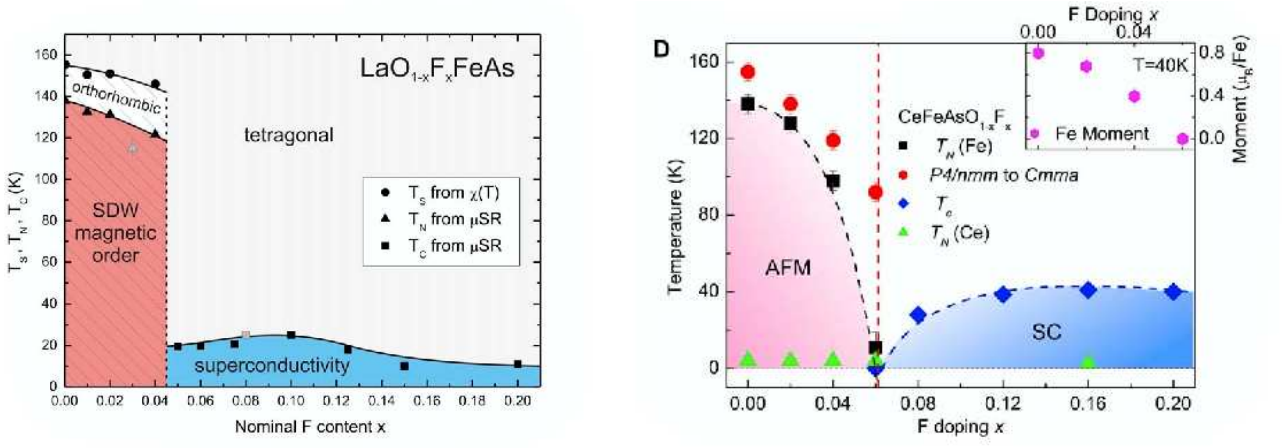

FIG. 9: (a) phase diagram of $LaO_{1-x}F_xFeAs$ obtained from μSR experiments [70]. It shows concentration dependence of critical temperatures of superconducting (T_c), magnetic (T_N) and structural transitions (T_s) (determined from resistivity measurements), (b) phase diagram of $CeO_{1-x}F_xFeAs$ system obtained from neutron scattering data in Ref. [71]. At the insert – concentration dependence of magnetic moment of Fe.

9 (b). According to this work, structural tetra – ortho transition ($P4/nmm \rightarrow Cmma$) is also well separated from antiferromagnetic transition, which takes place at lower temperatures, while superconductivity region does not overlap with the region of antiferromagnetic ordering on Fe. At the same time, magnetic structure of $CeO_{1-x}F_xFeAs$, shown in Fig. 10, is different from that of $LaO_{1-x}F_xFeAs$ (obtained by the same group [69]). In the $FeAs$ plane we again have a stripe – structure, similar to that in $LaOFeAs$, but spins on the adjacent planes are parallel and there is no period doubling along c axis. The value of magnetic moment on Fe is as high as $0.8(1)\mu_B$ at 40K, which is roughly twice as large as in $LaOFeAs$. Also in Ref. [71] a magnetic structure due to Ce spins ordering was determined at $T = 1.7$K. According to this work, strong correlation between spins of Fe and Ce appears already at temperatures below 20K. Note, that spin ordering on rare – earths in $REOFeAs$ series typically takes place at temperatures of the order of few K, which is nearly an order of magnitude higher than similar temperatures in cuprates like $REBa_2Cu_3O_{7-\delta}$ [72], giving an evidence of significantly stronger interaction of these spins. The general picture of spin ordering in $CeO_{1-x}F_xFeAs$ is shown in Fig. 10.

Note that data obtained by neutron scattering are still sometimes contradictory. For example, in Ref. [73], where $NdO_{1-x}F_xFeAs$ system was studied, it was claimed that spin ordering on Fe does not appear up to temperatures as low as $\sim$ 2K, when ordering of Fe and Nd spins takes place simultaneously, with the general picture of ordering similar to that shown in Fig. 10 for Fe and Ce. However, in Ref. [74] it was shown that antiferromagnetic ordering on Fe, similar to discussed above, in fact appears in $NdOFeAs$ at $T \sim 140$K, while difficulties with its observability are due, apparently, to rather small value of magnetic moment on Fe, which was found to be only 0.25 μ_B.

As to the phase diagram of 1111 systems, here also remain some questions. In Ref. [75] it was claimed that μSR data on $SmO_{1-x}F_xFeAs$ suggest an existence of some narrow region of coexistence of superconductivity and antiferromagnetism at doping levels 0.1¡x¡0.15. Naturally, the complete understanding of this situation will appear only in the course of further studies.

Neutronographic studies were also performed on different 122 compounds. Polycrystalline samples of $BaFe_2As_2$ were studied in Ref. [76]. It was shown that tetra – ortho structural transition ($I4/mmm \rightarrow Fmmm$) takes place practically at the same temperature $T_S \approx 142$K as antiferromagnetic transition, and spin ordering on Fe is the same as in 1111 systems, as shown in Fig. 11 (a). Magnetic moment on Fe at $T = 5$K is equal to 0.87(3) μ_B. Similar data were obtained also on the single – crystal of $SrFe_2As_2$ [77], where structural transition at $T_S = 220 \pm 1$K is very sharp, indicating, in authors opinion, the first – order transition. At the same temperature antiferromagnetic ordering of spins on Fe appears, of the same type as in $BaFe_2As_2$ (Fig. 11 (a)), and this transition is continuous. Magnetic moment on Fe at $T = 10$K is equal to 0.94(4) μ_B. These results unambiguously demonstrate the same nature of antiferromagnetic ordering of Fe spins in two – dimensional FeAs planes in 1111 and 122 systems.

In Ref. [78] a series of single crystals of $Ba_{1-x}K_xFe_2As_2$ with different x content were studied by X-ray, neutron scattering and electrical measurements. As a result, the authors have produced the phase diagram shown in Fig. 11 (b), where a region of coexistence of superconductivity and antiferromagnetism is clearly seen for $0.2 < x < 0.4$.

Concluding this section, let us note the recent work [79], where neutron scattering study was performed on α –

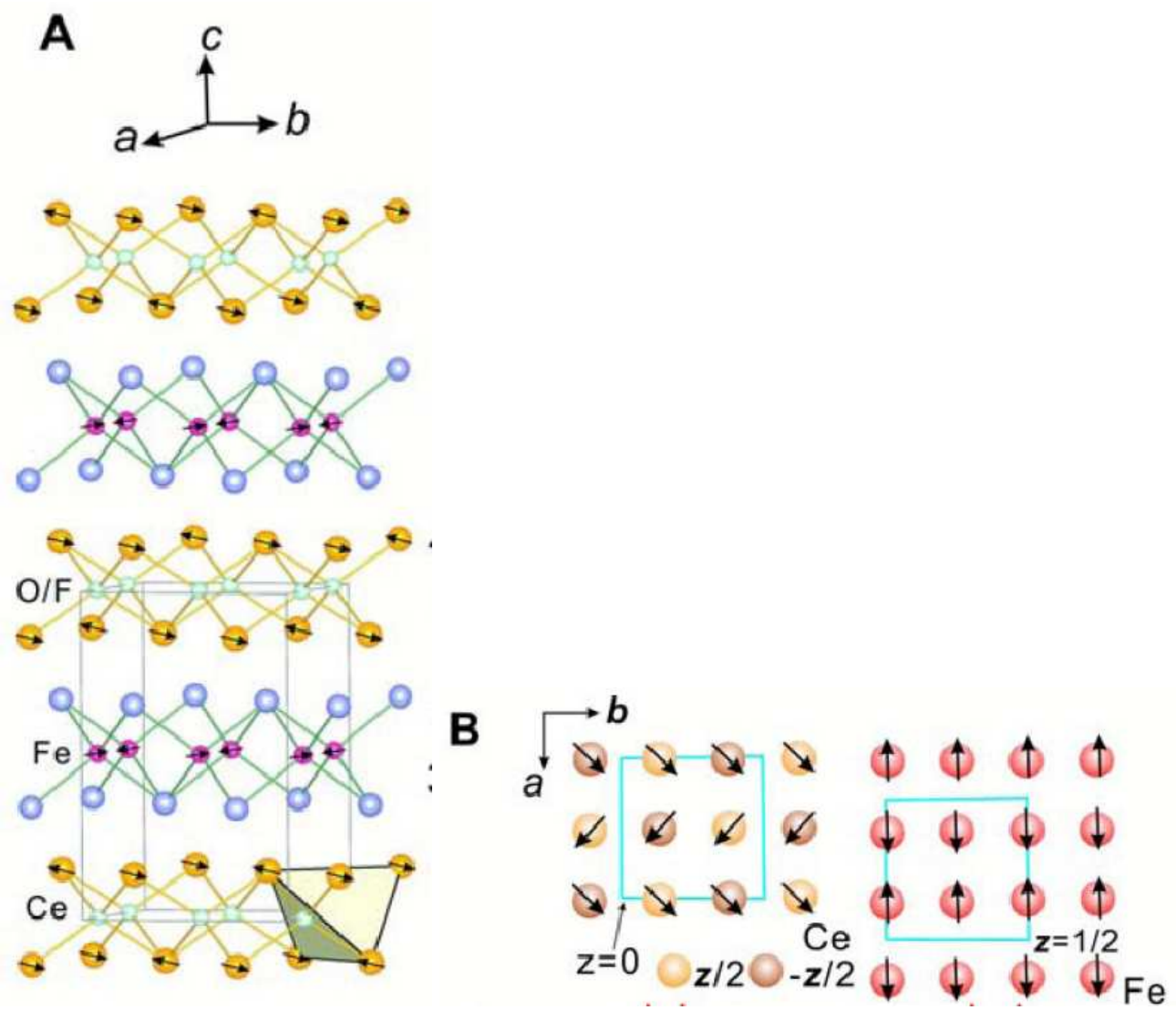

FIG. 10: Magnetic structure of CeOFeAs: (a) general picture of spin ordering at low temperatures, (b) magnetic elementary cells of Fe and Ce.

$Fe(Te_{1-x}Se_x)$ system for the first time. It was found that in the prototype $\alpha - FeTe$ (with excess of Fe) ordering of Fe spins takes place at temperatures lower than $T_S \approx 75$K (for $Fe_{1.076}Te$) and $T_S \approx 63$K (for $Fe_{1.141}Te$) and has a form of incommensurate spin density wave accompanied by structural transition from tetragonal to orthorhombic phase ($P4/nmm \rightarrow Pmmm$). Qualitative picture of spin ordering compared with the case of FeAs plane is shown in Fig. 12. At the same temperature T_S rather sharp anomaly is observed also in the temperature dependence of electrical resistivity. For superconducting composition $Fe_{1.080(2)}Te_{0.67(2)}Se_{0.33(2)}$ with $T_c \approx 14$K spin ordering and structural transition are absent, though well developed fluctuations of incommensurate SDW short – range order are observed.

Specific heat

Specific heat measurements in new superconductors were performed starting from the earliest works [30, 80]. As a typical example of specific heat behavior in 1111 systems consider $SmO_{1-x}F_xFeAs$ data of Ref. [80]. In Fig. 13 (a) we show temperature behavior of specific heat in this system for $x = 0$ and $x = 0.15$ (superconducting sample). An anomaly of specific heat is observed at $T_S \approx 130$K, which is obviously attributed to antiferromagnetic (SDW) (or structural tetra – ortho) transition. In superconducting sample ($x = 0.15$) this anomaly is absent. Besides this, in

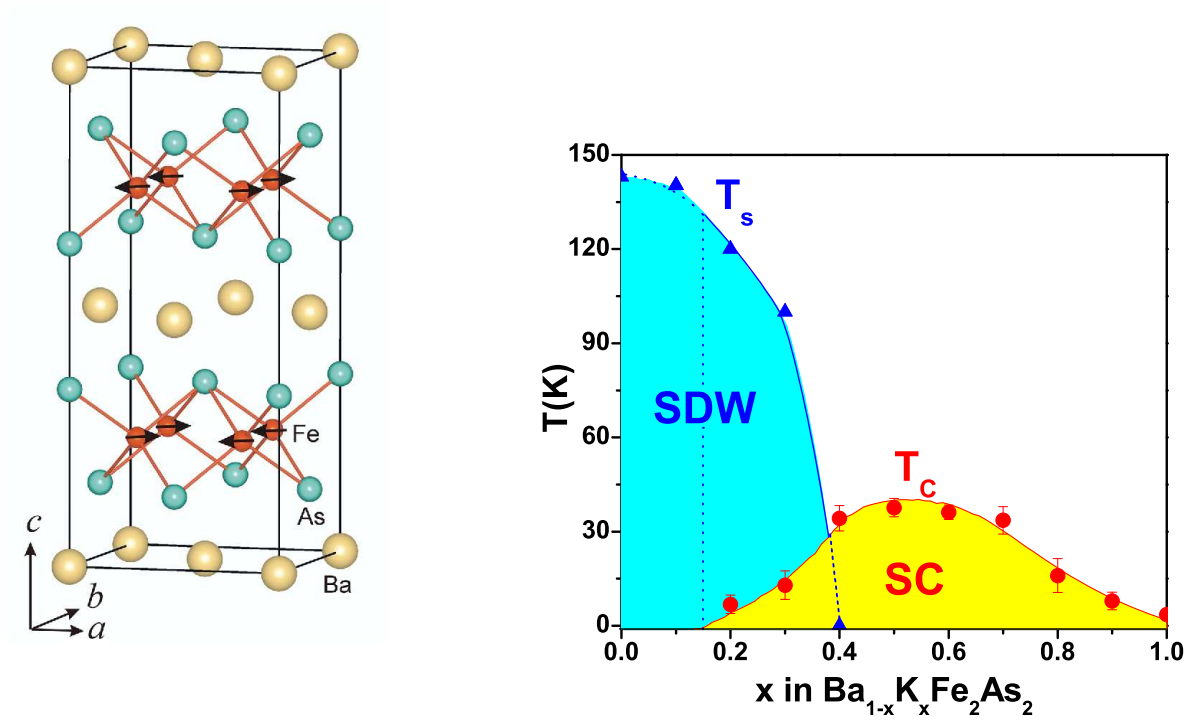

FIG. 11: (a) magnetic and crystal structure of $BaFe_2As_2$ in orthorhombic ($Fmmm$) cell [76], (b) phase diagram of $Ba_{1-x}K_xFe_2As_2$ according to Ref. [78]. T_S is the temperature of antiferromagnetic ordering (and structural transition), T_c is superconducting transition temperature.

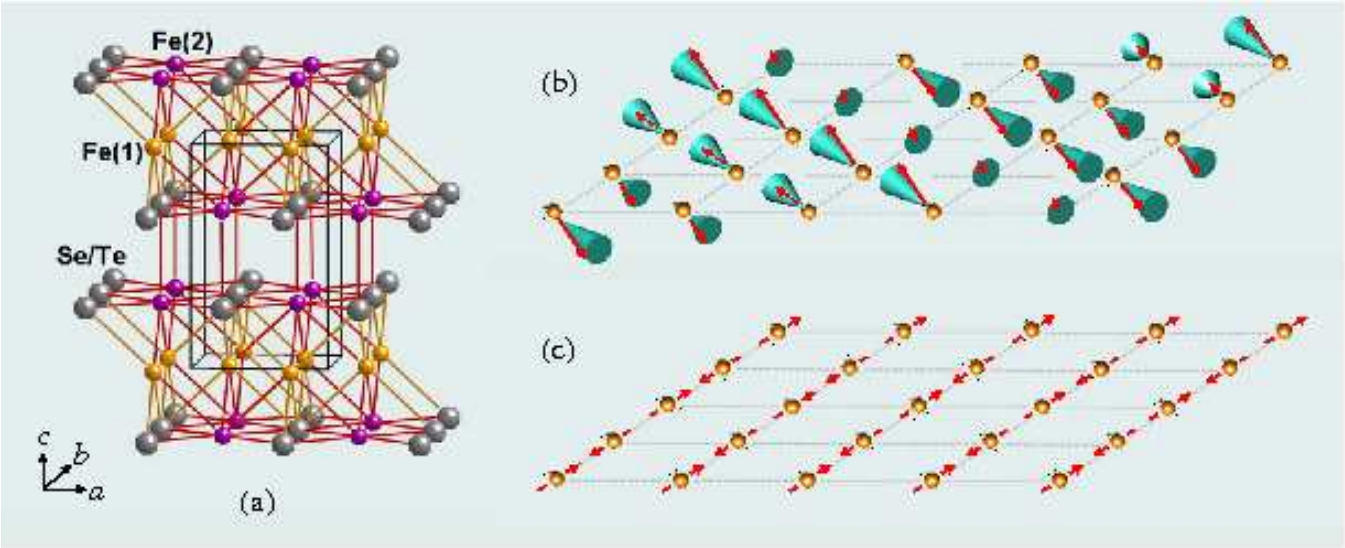

FIG. 12: (a) crystal structure of $\alpha - FeTe/Se$, excessive iron occupies positions Fe(2), (b) spin ordering in $\alpha - FeTe$ according to the data of Ref. [79] compared with antiferromagnetic ordering in $FeAs$ plane.

both samples there is a clear anomaly at $T \approx 5$K, which is connected with (antiferromagnetic) ordering of spins on Sm. As to specific heat discontinuity at superconducting transition, it is rather hard to separate, an is observed, according to Ref. [80], at temperatures significantly lower than superconducting T_c, determined by resistivity measurements.

Apparently, this is due to rather poor quality of samples (inhomogeneous content?).

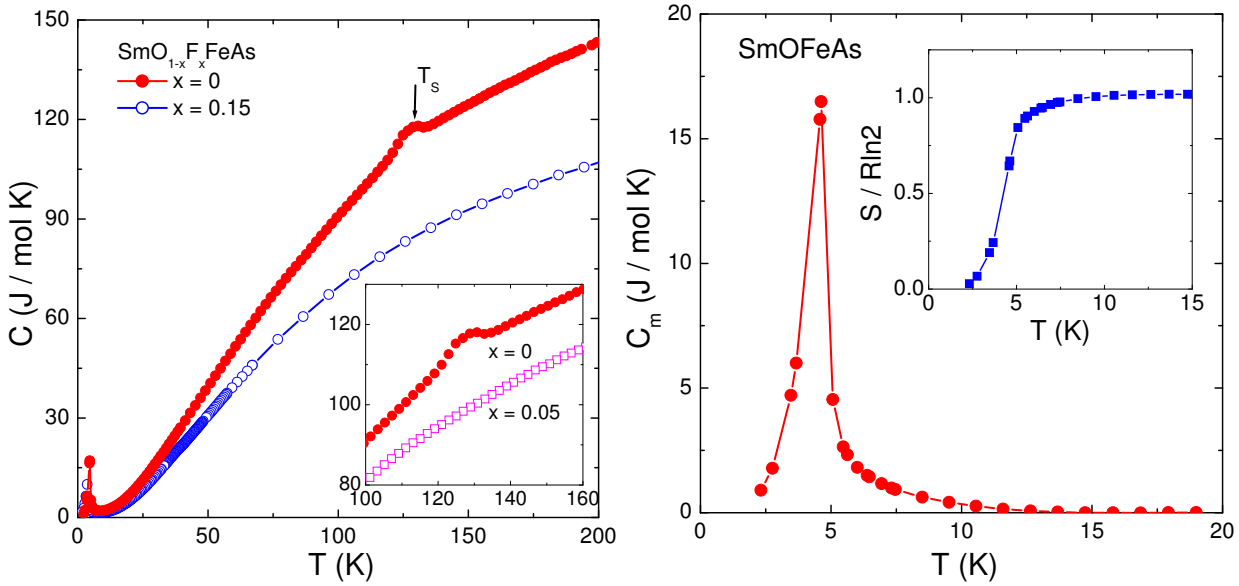

FIG. 13: (a) specific heat of $SmO_{1-x}F_xFeAs$ for $x = 0$ and $x = 0.15$ (superconducting sample) [80]. At the insert – region around $T_S = 130$K, where (for $x = 0$) an anomaly is observed, usually attributed to antiferromagnetic transition of spins on Fe, which is absent in superconducting sample, (b) magnetic contribution to specific heat of $SmOFeAs$ in the vicinity of Sm spins ordering temperature [80]. At the insert – entropy change due to this ordering.

In 122 systems studies of specific heat were done on single - crystalline samples [81, 82]. In Ref. 14 (a) we show temperature behavior of specific heat in superconducting single - crystal of $Ba_{0.6}K_{0.4}Fe_2As_2$ with $T_c = 35.8$K [82]. Detailed analysis allowed authors to separate and study electronic specific heat coefficient γ_n in the normal phase induced by magnetic field and in superconducting phase. Observed dependence of γ_n on the value of magnetic field allowed to come to a conclusion, that pairing in this system is of s – type, with non-zero energy gap everywhere at the Fermi surface (absence of gap zeroes characteristic e.g. for d-wave pairing in cuprates).

In Fig. 14 (b) a comparison is made of accurately separated electronic specific heat discontinuity ΔC_e at superconducting transition with predictions of BCS theory (weak coupling!). Agreement is quite impressing – the use of thus determined value of $\gamma_n \approx 63.3$ mJ/mol K^2 gives the value of $\Delta C_e/\gamma_n T|_{T=T_c} \approx 1.55$, to be compared with BCS theory prediction of 1.43. The fit to BCS theory allowed the authors to determine also the value of energy gap at low temperatures, which was found to be $\Delta_0 \approx 6$ meV. Below we shall see that this value is in good agreement with other data (ARPES).

NMR (NQR) and tunnelling spectroscopy

There are already a couple of studies of NMR (NQR) in new superconductors, leading to certain conclusions on the possible types of superconducting pairing in these systems. In Ref. [83] ^{75}As and ^{139}La NMR was studied in $LaO_{1-x}F_xFeAs$ for $x = 0.0, 0.04, 0.11$. In undoped $LaOFeAs$ a characteristic peak (divergence) of NMR relaxation $1/T_1$ on ^{139}La is observed at the temperature of antiferromagnetic transition $T_S \sim 142$K, while below the NMR spectrum is too wide, which is attributed to antiferromagnetic ordering. In superconducting sample with $x = 0.4$ ($T_c = 17.5$K) the value of $1/TT_1$ increases as temperature lowers up to ~ 30K following Curie – Weiss law: $1/TT_1 \sim C/(T + \theta)$ with $\theta \sim 10$K, with no divergence at finite temperatures, so that appearance of superconductivity is accompanied by suppression of magnetic ordering. The overall picture of nuclear spin relaxation for the sample with $x = 0.11$ ($T_c = 22.7$)K is qualitatively different. The value of $1/TT_1$ both on ^{139}La and ^{75}As decreases with lowering temperature, which is similar to NMR picture of pseudogap behavior in underdoped cuprates, approaching a constant in the vicinity of T_c, and is well fitted by activation temperature dependence with pseudogap value $\Delta_{PG} = 172 \pm 17$K [83].

In Fig. 15 (a) we show temperature dependence $1/T_1$ on ^{75}As in $LaO_{1-x}F_xFeAs$ system in superconducting state ($x = 0.04$ and $x = 0.11$) and in undoped $LaOFeAs$ (on ^{139}La nuclei, normalized according to $^{139}(1/T_1)/^{75}(1/T_1) \sim$

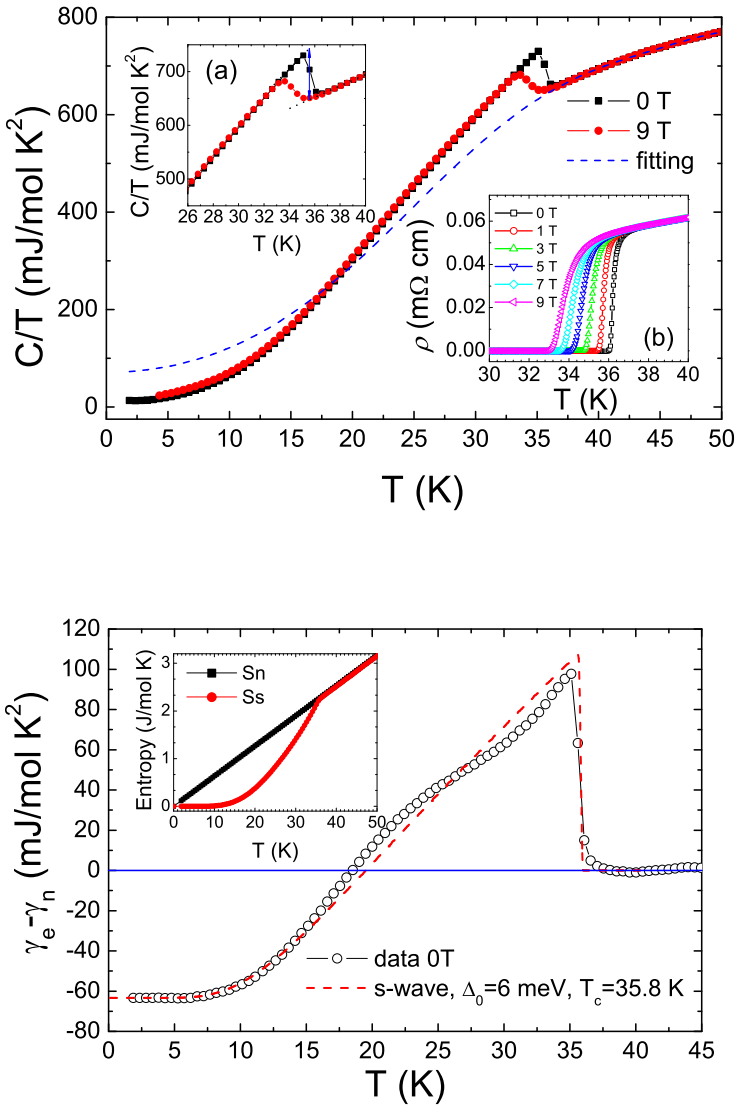

FIG. 14: (a) rough data on specific heat of $Ba_{0.6}K_{0.4}Fe_2As_2$ [82]. At the inserts – detailed behavior of specific heat in the vicinity of T_c and resistivity behavior close to superconducting transition in different magnetic fields, (b) electronic specific heat discontinuity and its comparison with predictions of BCS theory. At the insert – temperature behavior of entropy in normal and superconducting state [82].

0.135) [83]. Note the absence of Gebel – Slichter peak of $1/T_1$ in the vicinity of T_c and T^3 dependence of $1/T_1$ in superconducting region, characteristic for anomalous (non s – wave!) pairing with energy gap with zeroes on the Fermi surface, e.g. like in the case of d – wave pairing. In fact, these dependences are well fitted using $\Delta(\phi) = \Delta_0 \sin(2\phi)$, where ϕ is polar, angle determining direction of the momentum in two-dimensional inverse space, corresponding to $FeAs$ – plane, with the value of $2\Delta_0/T_c = 4.0$ [83].

Quite similar results were obtained in Ref. [84] during the studies of ^{75}As NMR and NQR in $LaO_{1-\delta}FeAs$ ($\delta = 0, 0.25, 0.4$) with T_c up to 28K and $NdO_{0.6}FeAs$ with $T_c = 53$K. In particular, these authors has come to a conclusion that their NQR relaxation data for $LaO_{0.6}FeAs$ in superconducting phase, correspond to an energy gap of the form $\Delta = \Delta_0 \cos(2\phi)$ with $\frac{2\Delta_0}{T_c} \approx 5$, which corresponds to d – wave pairing with gap zeroes at the Fermi surface, i.e. the same pairing symmetry as in cuprates. Temperature behavior of $1/T_1$ for $T > T_c$, found in this work, also gives an evidence of pseudogap behavior with pseudogap value $\Delta_{PG} \approx 196$K.

In Ref. [85] ^{75}As Knight shift measurements were done in $PrO_{0.89}F_{0.11}FeAs$. The sharp drop of Knight shift

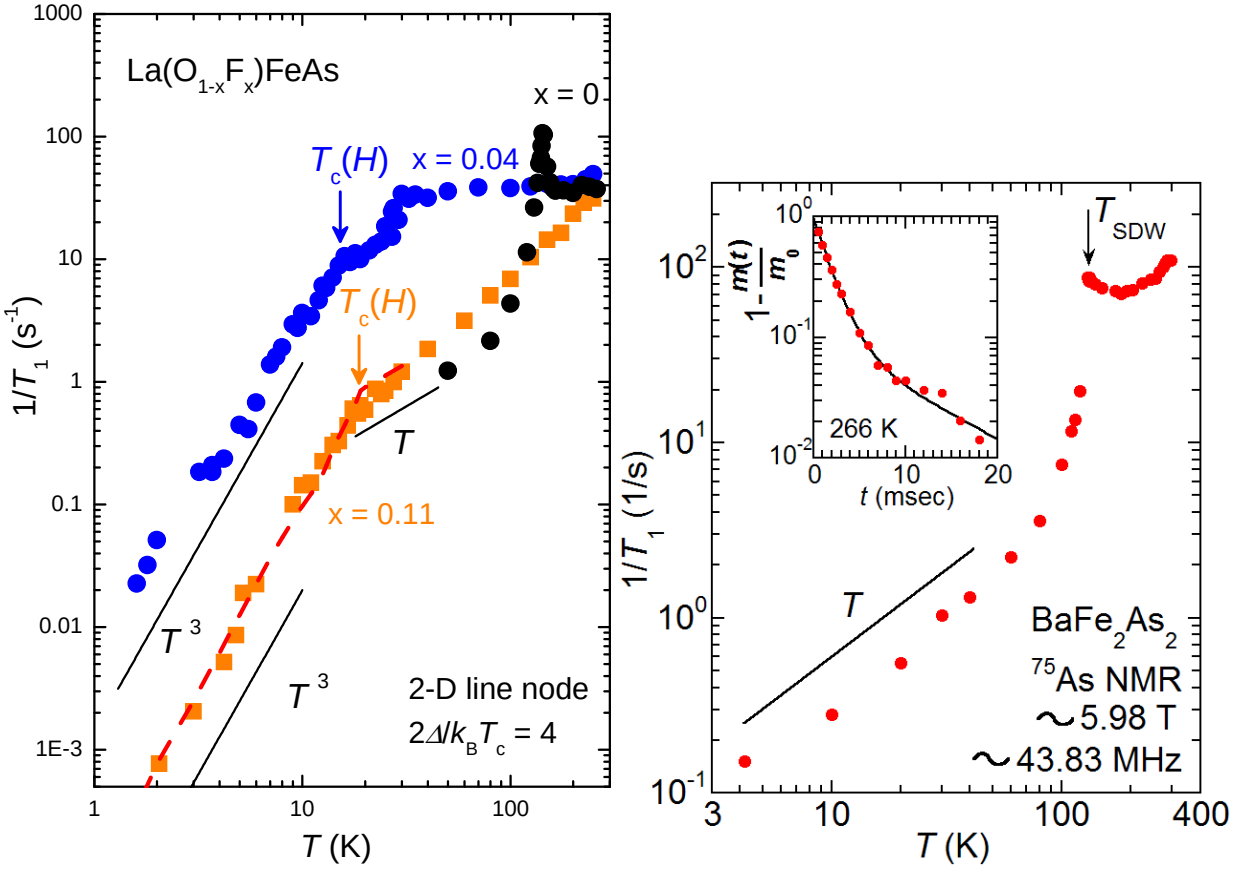

FIG. 15: (a) temperature dependence of NMR relaxation rate $1/T_1$ in $LaO_{1-x}F_xFeAs$ for $x = 0.0, 0.04, 0.11$ in low temperature region of the order of T_c and below [83], (b) temperature dependence of $1/T_1$ ^{75}As in undoped $BaFe_2As_2$ [86].

for $T < T_c$ is a definite evidence of singlet nature of pairing. Details of temperature dependence of Knight shift were well fitted using the model with two d-wave superconducting gaps: $\Delta = \Delta_0 \cos(2\phi)$, $\Delta_0 = \alpha\Delta_1 + (1-\alpha)\Delta_2$ with $2\Delta_1/T_c \approx 7$ $2\Delta_2/T_c \approx 2.2$, $\alpha = 0.4$. In the same model the authors of Ref. [85] has successfully described temperature dependence of $1/T_1$ on ^{19}F for $T < T_c$.

NMR study of undoped $BaFe_2As_2$ was performed in Ref. [86]. The temperature dependence of $1/T_1$ is shown in Fig. 15 (b). A clear anomaly is observed at $T = 131$K, connected to antiferromagnetic (SDW) transition. Sharp drop of $1/T_1$ is attributed to SDW – gap opening at the part of Fermi surface. Linear over T behavior of relaxation rate for $T < 100$K is due to relaxation of nuclear spins on conduction electrons, remaining on the "open" parts of Fermi surface. In general, situation here is reminiscent of similar behavior in $LaOFeAs$, though there are some significant quantitative differences [86].

NMR study of superconducting phase in 122 system was done on $BaFe_{1.8}Co_{0.2}As_2$ with $T_c = 22$K in Ref. [87]. In Fig. 16 results on nuclear spin relaxation rate and Knight shift are shown. For temperatures below 280K a drop of $1/TT_1$ is observed, which is approximated by activation dependence with (pseudo)gap $\Delta_{PG} \approx 560$K (Fig. 16 (b)), which is significantly larger than pseudogap width estimates for $LaO_{0.9}F_{0.1}FeAs$ obtained in Ref. [83] and quoted above. Data on Knight shift (Fig. 16 (c)), similarly to 1111 case, give an evidence of singlet pairing. Temperature dependence of Knight shift above T_c also show pseudogap behavior with the same pseudogap width as obtained from fitting the data on relaxation rate.

Thus NMR data on 1111 and 122 systems are in many respects similar. Singlet pairing follows unambiguously, asa well as an evidence for the anomalous nature of pairing with probable gap zeroes on the Fermi surface (and probably the presence of two superconducting gaps). However, below we shall see that the conclusion on gap zeroes contradicts some other experiments and interpretation of NMR data may be quite different.

As to $\alpha - FeSe$ system, up to now there is only one NMR study on $FeSe_{0.92}$ with $T_c = 8$K [88] (NMR on ^{77}Se nuclei), demonstrating the absence of Gebel – Slichter peak in the temperature dependence of $1/T_1$ in the vicinity of T_c and also the absence of any anomaly which can be attributed to any kind of magnetic ordering at higher temperatures,

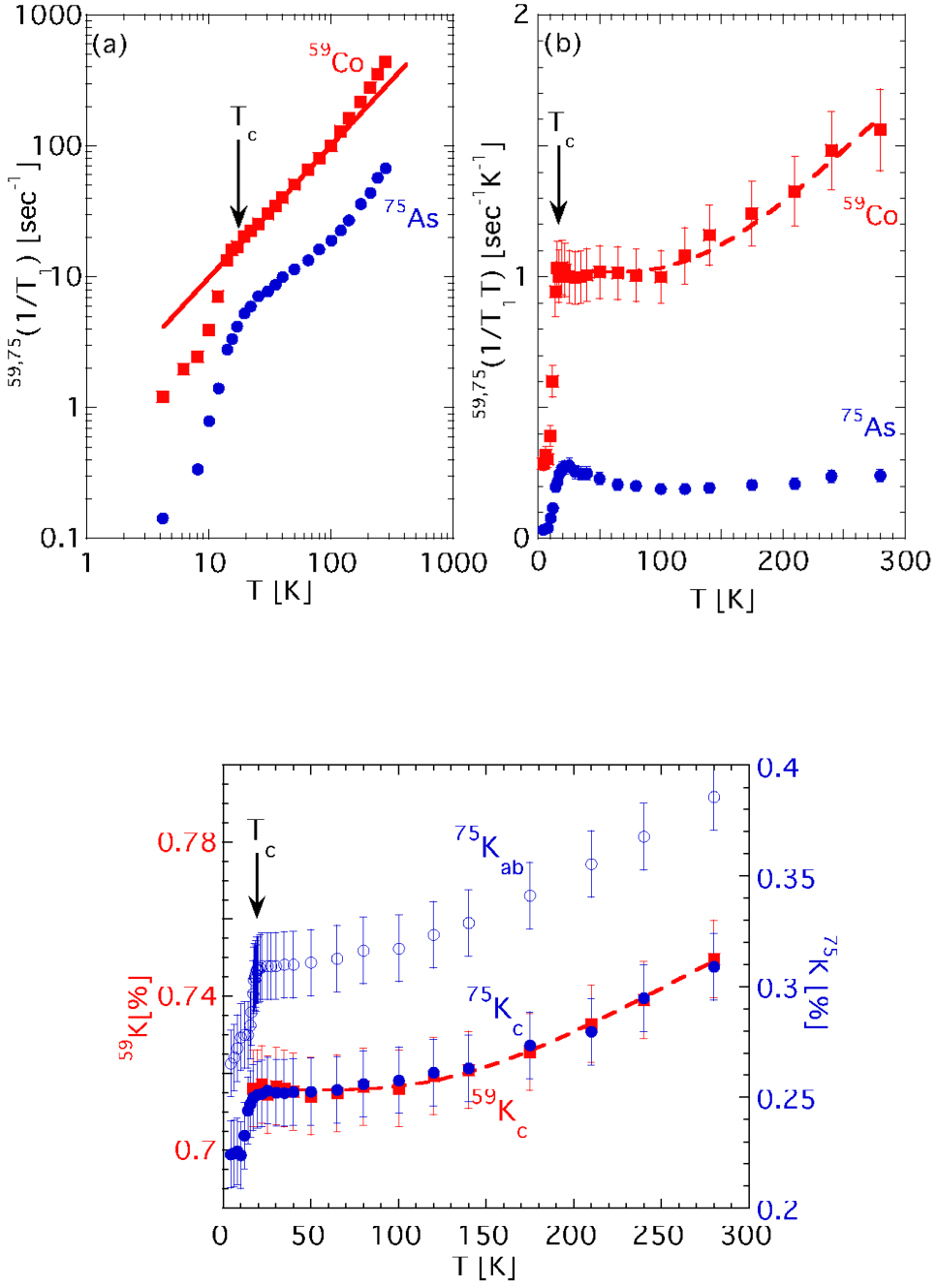

FIG. 16: (a) temperature dependence of $1/T_1$ on ^{59}Co and ^{75}As in $BaFe_{1.8}Co_{0.2}As_2$ and similar dependence of $1/TT_1$ (b), where dashed curve corresponds to activation dependence with pseudogap $\Delta_{PG} = 560 \pm 150$K [87], (c) temperature dependence of Knight shift on ^{59}Co and ^{75}As in the same system, where dashed curve is described by activation dependence with the same pseudogap width.

as well as the absence there of any kind of "pseudogap" behavior (validity of Korringa relation). At the same time, in the $T < T_c$ region $\sim T^3$ – behavior of $1/T_1$ is observed, probably giving an evidence for zeroes of superconducting gap at the Fermi surface.

Among a number of studies using different kinds of tunnelling spectroscopy, let us mention Refs. [89, 90, 91]. Up to now these experiments were performed on polycrystalline samples and results are somehow contradictory.

In Ref. [89] the method of Andreev spectroscopy was applied to $SmO_{0.85}F_{0.15}FeAs$ with $T_c = 42$K. Only one superconducting gap was observed with $2\Delta = 13.34 \pm 0.3$ meV (close to $T = 0$), which corresponds to $2\Delta/T_c = 3.68$, i.e. quite close to a standard BCS value of 3.52. Temperature dependence of the gap, determined in Ref. [89], also closely followed BCS theory. In authors opinion, these results give an evidence of the usual (s-wave) order parameter with no zeroes at the Fermi surface, in obvious contradiction with NMR results quoted above.

In Ref. [90] similar system – $SmO_{0.85}FeAs$ with $T_c = 52$K was studied by scanning tunnelling spectroscopy at $T = 4.2$K. Good quality tunnelling characteristics were obtained only from some parts of the sample surface, and these were fitted to tunnelling characteristics of d-wave superconductor with $\Delta = 8 \div 8.5$ meV, which corresponds to $2\Delta/T_c \sim 3.55 \div 3.8$.

The same method of scanning tunnelling spectroscopy (microscopy) was applied also in Ref. [91] to $NdO_{0.86}F_{0.14}FeAs$ with $T_c = 48$K, and measurements were done at different temperatures. At temperatures significantly lower than T_c on different parts of sample surface two gaps were observed – a bigger one $\Delta \sim 18$ meV and smaller $\Delta \sim 9$ meV. Both gaps closed at the transition point $T = T_c$, with smaller gap more or less following the BCS temperature dependence. At the same parts of the surface, where the smaller gap was observed below T_c, slightly above T_c a jumplike opening pseudogap appeared closing only at $T = 120$K. At present there is no clear interpretation of this unexpected behavior.

Note also Ref. [92] where $SmO_{0.9}F_{0.1}FeAs$ with $T_c = 51.5$K was studied by point contact spectroscopy. The authors also observed two superconducting gaps – a larger one $\Delta = 10.5 \pm 0.5$ meV and smaller one $\Delta = 3.7 \pm 0.4$ meV, with both gaps following BCS – like temperature dependence.

Up to now there are no systematic tunnelling data for 122 systems.

Contradictory nature of existing data of tunnelling spectroscopy is more or less obvious. It seems we have to wait the results of experiments on single crystals.

Optical properties

The measurements of optical properties of new superconductors were done in a number of works, both on polycrystalline samples of 1111 systems 1111 [93, 94] and on single crystals of 122 system [95, 96].

In Ref. [93] ellipsometry measurements of dielectric permeability of $REO_{0.82}F_{0.18}FeAs$ ($RE = Nd, Sm$) were made in the far infrared region. It was shown that electronic properties of these systems are strongly anisotropic (quasi two-dimensional) and, in these sense, analogous to those of cuprates. A noticeable suppression of optical conductivity in superconducting state was discovered, which was attributed by the authors to the opening of superconducting gap $2\Delta \approx 300\text{cm}^{-1}$ (37 meV), corresponding to $2\Delta/T_c \sim 8$, i.e. the strong coupling limit.

In Ref. [94] the same method was applied to the studies of dielectric permeability of $LaO_{0.9}F_{0.1}FeAs$ with $T_c = 27$K in a wide frequency interval of $0.01 \div 6.5$ eV at temperatures $10 \leq T \leq 350$K. Unusually narrow region of Drude behavior was observed, corresponding to the density of free carriers as low as 0.040 ± 0.005 per unit cell, as well as signatures of pseudogap behavior at 0.65 eV. Besides that, the authors have also observed a significant transfer of spectral weight to the frequency region above 4 eV. These results allowed to conclude that electronic correlations (and (or) electron – phonon coupling) are very important in these systems.

The studies of reflectance and real part of optical conductivity of a single crystal of $Ba_{0.55}K_{0.45}Fe_2As_2$ [95] has shown that the absorption spectrum of this system consists of a noticeable Drude peak at low frequencies and a wide absorption band with maximum at 0.7 eV, which the authors attributed to carrier scattering by collective (Boson) excitations (e.g. spin fluctuations) with energies of the order of 25 meV and strongly temperature dependent coupling constant (with carriers).

Most convincing and interesting optical data were obtained in Ref. [96], where detailed measurements of reflectance were performed on the single crystal of $Ba_{0.6}K_{0.4}Fe_2As_2$ with $T_c = 37$K in the infrared region and in the wide temperature interval $10 \div 300$K.

In Fig. 17 we show the data on real part of optical conductivity $\sigma_1(\omega)$ obtained in Ref. [96]. It is seen that close to and below T_c (curves, corresponding to 27 K and 10 K) demonstrate rapid drop of $\sigma_1(\omega)$ at frequencies below 300 cm^{-1}, so that conductivity is practically zero below 150 cm^{-1}, which gives an evidence of superconducting s – wave gap opening. Gap value determined by absorption edge is $2\Delta \simeq 150$ cm^{-1}, which correlates well with ARPES data to be discussed below.

Thus, at temperatures significantly lower T_c a considerable suppression of low frequency conductivity is observed, which is connected with the formation of condensate of Cooper pairs. According to the well known Ferrell–Glover–

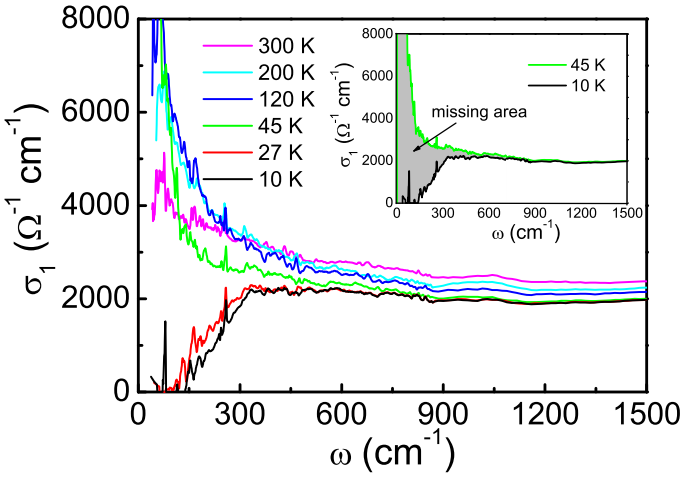

FIG. 17: Real part of optical conductivity of $Ba_{0.6}K_{0.4}Fe_2As_2$ at different temperatures [96]. At the insert – comparison of the data at 10K and 45K, where the "missing area", connected with superconducting gap opening and formation of condensate of Cooper pairs is clearly seen.

Tinkham sum rule [97, 98] the difference of conductivities at T$\simeq T_c$ and T$\ll$T$_c$ (i.e. the so called "missing area" between appropriate curves, shown at the insert in Fig. 17) directly determines the value of condensate density via:

$$\omega_{ps}^2 = 8\int_{0+}^{\omega_c}[\sigma_1(\omega, T \simeq T_c) - \sigma_1(\omega, T \ll T_c)]d\omega \qquad (1)$$

where $\omega_{ps}^2 = 4\pi n_s e^2/m^*$ – is the square of plasma frequency of superconducting carriers, n_s is the their density, and ω_c – is a cut-off frequency, which is chosen to guarantee the convergence of ω_{ps}^2. Then we can determine the penetration depth as $\lambda = c/\omega_{ps}$. Eq. (1) defines (via the general optical sum rule) the fraction of electron (carrier) density, which is transferred to $\delta(\omega)$ singularity of $\sigma_1(\omega)$, corresponding to superconducting response of the condensate. Direct estimate of the value of "missing area" gives for penetration depth the value λ=2080 Å, which agrees well with other data [96].

Phonons and spin excitations: neutron spectroscopy

Up to now a number of experiments have already been done to study collective excitations, i.e. phonons and spin waves, in new superconductors, which is of principal importance for the clarification of the nature of Cooper pairing in these systems. Below we shall mainly deal with experiments on inelastic neutron scattering.

In Ref. [99] inelastic neutron scattering was studied on $LaO_{0.87}F_{0.13}FeAs$ with $T_c \approx$ 26K. Characteristic maxima of phonon density of states were observed at 12 and 17 meV.

In more details phonon density of states in $LaO_{1-x}F_xFeAs$ (for $x = 0$ and $x \sim 0.1$) was studied in Ref. [100], where it was also compared with results of phonon spectrum calculations done in Ref. [101]. Main results of this work are shown in Fig. 18 (a-c), where we can see both the general structure of phonon density of states and a satisfactory agreement with calculations of Ref. [101]. Also we can observe that the phonon spectrum of prototype 1111 system is differs very little from that observed in doped (superconducting) sample. The origin of peaks in phonon density of states is well explained on the basis of theoretical calculations.

Phonon density of states in 1111 systems was also studied by nuclear resonance inelastic synchrotron radiation scattering [102] (in systems based on La) as well as by inelastic X-ray scattering [103] (systems based on La and Pr). In all cases, results found are quite similar to that obtained by inelastic neutron scattering and are in satisfactory agreement with theoretical calculations.

As to 122 systems, up to now there are works on inelastic neutron scattering on the prototype system $BaFe_2As_2$ [104, 105], where consistent results were obtained, which are also in agreement with results of theoretical calculations of phonon spectrum made in these works. As an example, in Fig. 18 (d) we show a comparison of calculated and experimental phonon densities of states for this system made in Ref. [104]. We see quite satisfactory agreement, except an additional peak at frequency of the order of 21.5 meV, observed in the experiments.

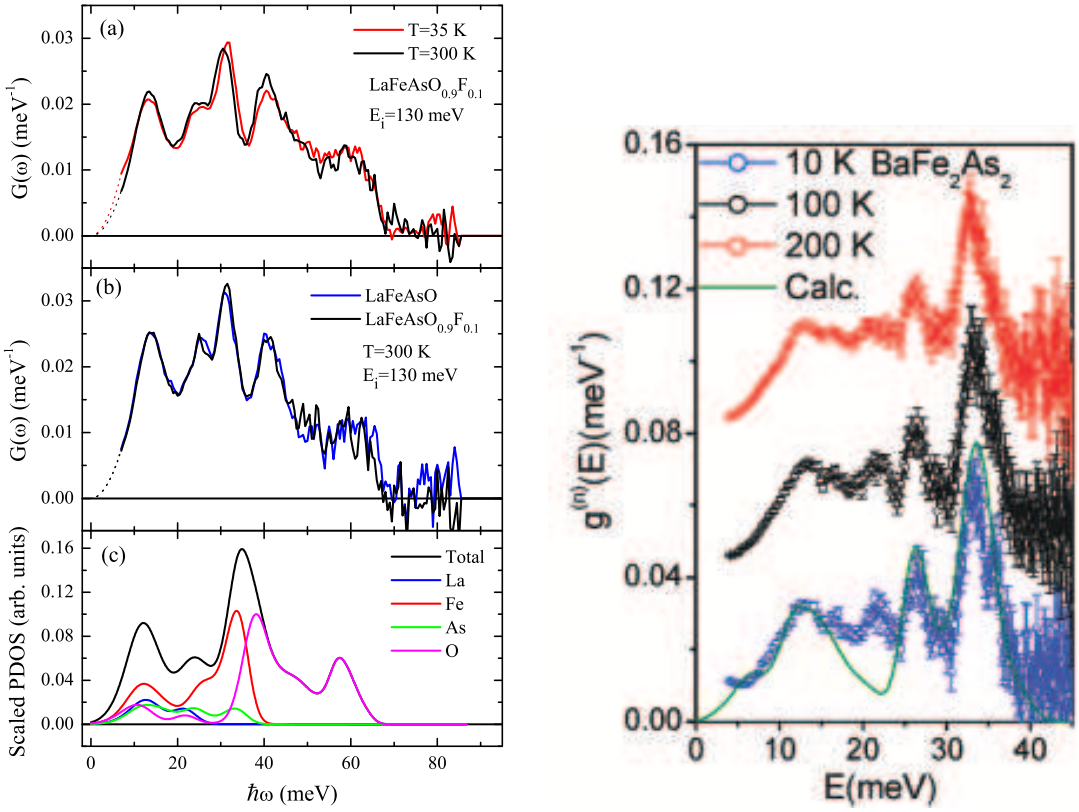

FIG. 18: (a)-(b) phonon density of states in $LaO_{1-x}F_xFeAs$, obtained from inelastic neutron scattering [100] and compared with calculated () in Ref. [101], (d) comparison of experimental and calculated phonon density of states in $BaFe_2As_2$ [104].

Dynamics of spin excitations in new superconductors was studied by neutronography in $SrFe_2As_2$ [106] and $BaFe_2As_2$ [107], i.e. on undoped samples, where antiferromagnetic ordering takes place at low temperatures.

In particular, in Ref. [106] it was shown that the spectrum of magnetic excitations is characterized by a gap $\Delta \leq 6.5$ meV, while above this gap the well defined spin waves are observed, and the measurement of their velocity allowed to estimate exchange integrals (in localized spins model). In the vicinity of the temperature of antiferromagnetic transition no signs of critical scattering was observed, which in the opinion of authors show that magnetic transition here is of the first order [106].

Qualitatively similar results (though without detailed measurements of spin wave dispersion) were obtained in Ref. [107], where it was shown that magnon spectrum continues up to energies, which are significantly higher than typical phonon frequencies ($\sim$ 40 meV) and ends at energies about 170 meV.

Other experiments

In our rather short review of experiments on new superconductors we could not pay attention to a number of important studies. Outside our presentation remained more detailed discussion of experiments on critical magnetic fields (in particular measurements of H_{c1}), direct measurements of penetration depth, experiments on X-ray photoemission. Practically we have not paid any attention to experiments on traditional transport properties in the normal state (such as Hall effect, thermoelectricity etc.). It is connected mainly with the limited size of this review, as well as by personal preferences of the author. Below, in theoretical part of this review we shall return to discussion of a number of extra experiments. In particular, we shall pay much attention to experiments of angle resolved photoemission (ARPES), which are more appropriately discussed in parallel with discussion of electronic spectrum of these systems. The same applies to some other experiments on determination of Fermi surfaces (quantum oscillation effects in strong magnetic fields).

ELECTRONIC SPECTRUM AND MAGNETISM

Band structure (LDA)

Clarification of the structure of electronic spectrum of new superconductors is crucial for explanation of their physical properties. Accordingly, since the first days, different groups have started the detailed band – structure calculations for all classes of these compounds, based primarily on different realizations of general LDA approach.

First calculations of electronic spectrum of iron oxypnictide $LaOFeP$ were performed in Ref. [108], before the discovery of high temperature superconductivity in FeAs based systems. For $LaOFeAs$ such calculations were, almost simultaneously, were done in Refs. [101, 109, 110, 111]. In the following, similar calculations were performed also for the other 1111 systems, as well as for 122 [112, 114], 111 [113, 114, 115] and α-FeSe [116]. As results obtained in all these references were more or less similar, in the following we shall concentrate in more details on our group works [117, 118, 119, 120], referring to other authors where necessary. We shall also limit ourselves mainly to the results obtained for nonmagnetic tetragonal phase of 1111 and 122 systems (as well as 111), as superconductivity is realized in this phase.

In Ref. [117] we have performed *ab initio* calculations of electronic structure for a number of oxypnictides from the series $REO_{1-x}F_xFeAs$ (where RE=La, Ce, Nd, Pr, Sm, and also for the hypothetical at a time case of RE=Y) in the framework of the standard LDA-LMTO approach [122].

In Fig. 19 (a) we show the comparison of electronic spectra of $LaOFeAs$ and $PrOFeAs$ [117] in main symmetry directions in Brillouin zone. It can be seen that differences in spectra due the change of rare – earth ion (as well as a small change in lattice constants) are rather small. In a narrow enough energy interval close to the Fermi energy, which is relevant to superconductivity (of the order of $\pm$ 0.2 eV), these spectra practically coincide.

This is also clearly seen from the comparison of the densities of states shown in Fig. 19 (b). In fact, densities of states of both compounds close to the Fermi level are just the same (up to few percents). This is typical also for the other compounds from the rare – earth series $REO_{1-x}F_xFeAs$ [117].

The only noticeable difference in spectra of these systems with different rare – earth ions manifests itself in the growth of tetrahedral splitting due to lattice compression, which appears at energies of the order of -1.5 eV for d-states of Fe and -3 eV for p-states of As.

From comparison of partial densities of states we can also see that the value of the density of states close to the Fermi level is determined almost entirely by d-states of Fe (with very insignificant contribution from p-states of As). In this sense we can say that all phenomena related to superconductivity in these compounds take place in the square lattice of Fe within FeAs layer.

Naturally, most of these peculiarities of electronic spectra can be attributed to the quasi – two – dimensional character of compounds under study. For example, the insensitivity of electronic spectra to the type of rare – earth ion is simply due to the fact that electronic states of REO layers are far from the Fermi level and p-states of O only weakly overlap with d-states of Fe and p-states of As in FeAs layers. Accordingly, hybridization of d-states of Fe and p-states of As is more significant, but still is not very strong, as demonstrated by band structure calculations.

Thus, situation with rare – earth substitutions in REOFeAs series seems to be largely analogous to the similar one in cuprates like $REBa_2Cu_3O_{7-x}$, which were studied in the early days of HTSC research [72, 123]. In these compounds electronic states of rare – earth ions also do not overlap with electronic states in conducting CuO_2 planes, which leads to the well known fact of almost complete independence of superconducting $T_c \sim 92K$ on the type of rare – earth RE=Y,Nd,Sm,Eu,Gd,Ho,Er,Tm,Yb,Lu,Dy [123], with only two exceptions – that of much lower $T_c \sim 60K$ in case of La and complete absence of superconductivity in case of Pr based compound [72].

Similarly, almost identical electronic structure of iron oxypnictides like REOFeAs with different RE in a wide enough energy interval around the Fermi level seems to lead inevitably to approximately the same values of superconducting transition temperature T_c (in any BCS – like microscopic mechanism of pairing). Different rare – earth ions just do not influence electronic structure, at least in this energy interval around the Fermi level, and, accordingly, do not change the value of the pairing coupling constant. Also, there is no special reasons to believe that the change of rare – earth ion will change much the phonon spectrum of these systems, as well as the spectrum of magnetic excitations in FeAs layer.

Thus, we have a kind of rare – earth puzzle — in contrast to cuprate series $REBa_2Cu_3O_{7-x}$ different rare – earth substitutions in REOFeAs series lead to rather wide distribution of T_c values, from $\sim$ 26K in case of La system to $\sim$ 55K in case of Nd and Sm. At the moment we can propose two possible explanations of this puzzle:

1. Different quality of samples (disorder effects) can lead to rather wide distribution of T_c values, as internal disorder can strongly influence on the value of critical temperature, especially in case of anomalous pairings

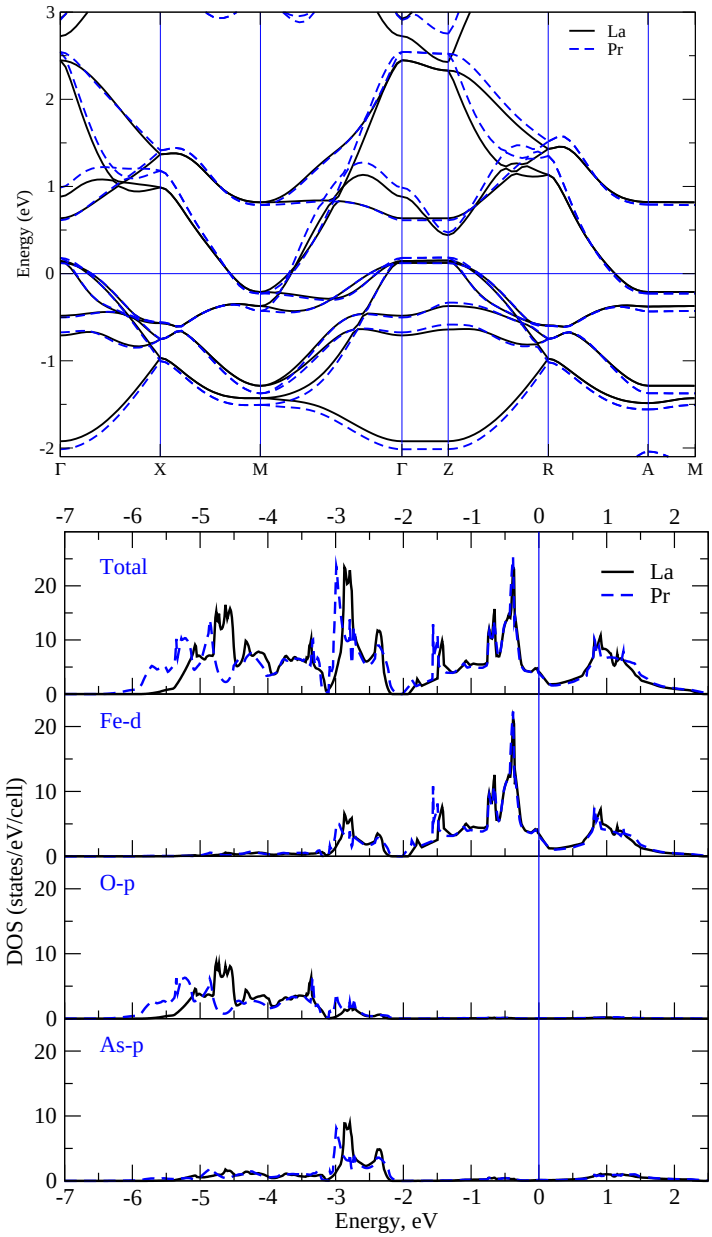

FIG. 19: (a) electronic spectra of $LaOFeAs$ and $PrOFeAs$ in high - symmetry directions in the Brillouin zone of tetragonal lattice, obtained in LDA approximation citeNek1239, (b) comparison of the total and partial densities of states in $LaOFeAs$ and $PrOFeAs$ [117].

(anisotropic s - wave, even more so p or d-wave pairing, triplet pairing etc.), which are widely discussed at present for FeAs superconductors [110, 124]. This possibility is qualitatively analogous to the case of copper oxides, where d-wave pairing is realized, which is strongly suppressed by disorder. This argumentation was used e.g. to explain lower values of T_c in $LaBa_2Cu_3O_{7-x}$, which were attributed to disorder in positions of La and Ba ions, as well as to oxygen vacancies [72]. In fact, this point of view is confirmed by the reports on the synthesis of $LaO_{1-x}FeAs$ with $T_c \sim 41$K [34], as well as by the synthesis of initially hypothetical [117] $YO_{1-x}FeAs$ system, first with $T_c \sim 10$K [125], and later (synthesis under high pressure) with $T_c \sim 46$K [126]. In this last paper 1111 compounds based on Ho, Dy and Tb were also synthesized, leading to T_c values of the order of 50, 52 and 48K correspondingly. It seems quite probable that the best prepared samples of 1111 series may achieve the values of $T_s \sim 55$K, as obtained in most "favorable" cases of Sm and Nd. This stresses the necessity of systematic studies of disorder effects in new superconductors.

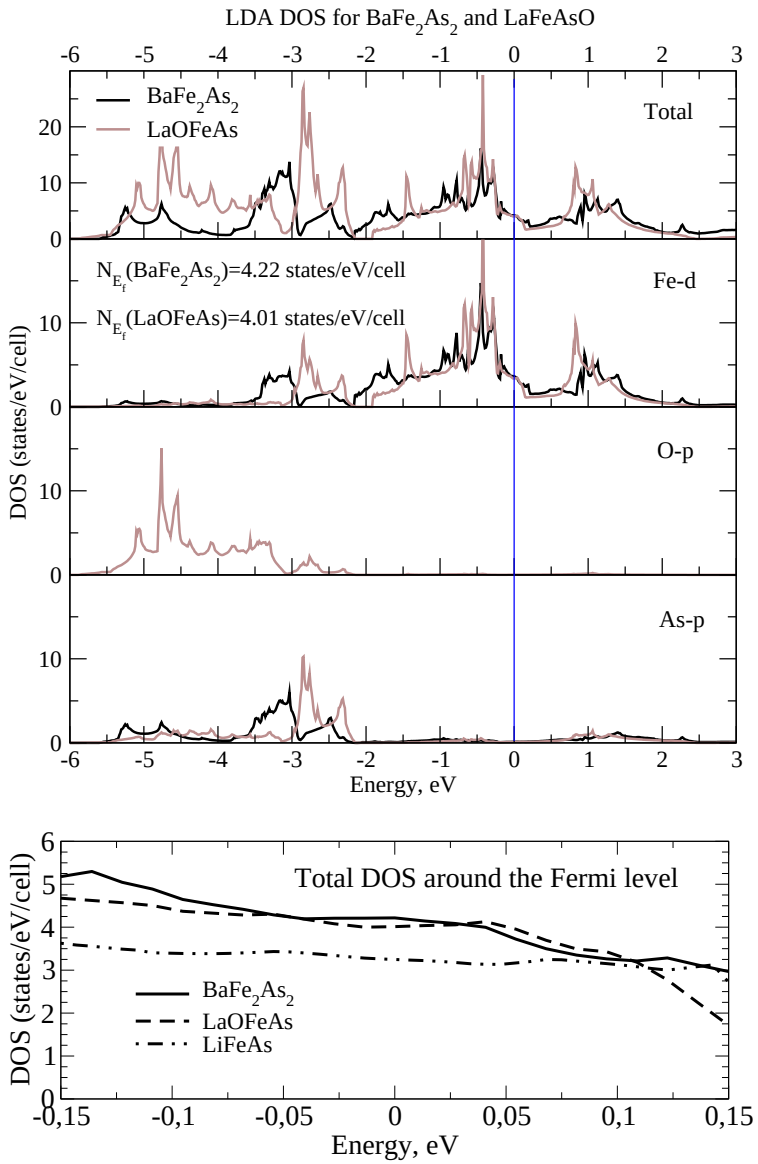

FIG. 20: (a) comparison of the total electronic density of states and partial densities of states in $LaOFeAs$ and $BaFe_2As_2$ [118], (b) comparison of densities of states in a narrow energy interval around the Fermi level in $LaOFeAs$, $BaFe_2As_2$ and $LiFeAs$ [119].

2. However, we cannot exclude also the other physical reasons of T_c distribution in REOFeAs series, connected e.g. with spin ordering on rare – earth ions (like Ce, Pr, Nd, Sm, Gd, which possess magnetic moments). Above we have already mentioned the unusually high coupling of these moments with moments on Fe. Besides, the temperature of rare – earth moments ordering is known experimentally to be an order of magnitude higher than in $REBa_2Cu_3O_{7-x}$ systems [72], which also indicates to rather strong magnetic couplings, which may significantly influence e.g. on spin fluctuation spectrum in FeAs layers (and T_c values in case of magnetic mechanisms of pairing [110, 124]).

In Fig. 20 (a) we show the comparison of total electronic density of states and partial densities of states in $LaOFeAs$ and $BaFe_2As_2$ [118]. It is seen that again we have almost the same values of DOS'es in an energy interval around the Fermi level, relevant to superconductivity. In more details we can see it in Fig. 20 (b), where densities of states are compared in a narrow energy interval ($\pm$ 0.15 eV) close to the Fermi level in $LaOFeAs$, $BaFe_2As_2$ and $LiFeAs$ [119]. The densities of states in this energy interval are almost energy independent (quasi two – dimensionality!) and only slightly different (though, in principle, we can notice some correlation of these values of DOS at the Fermi level

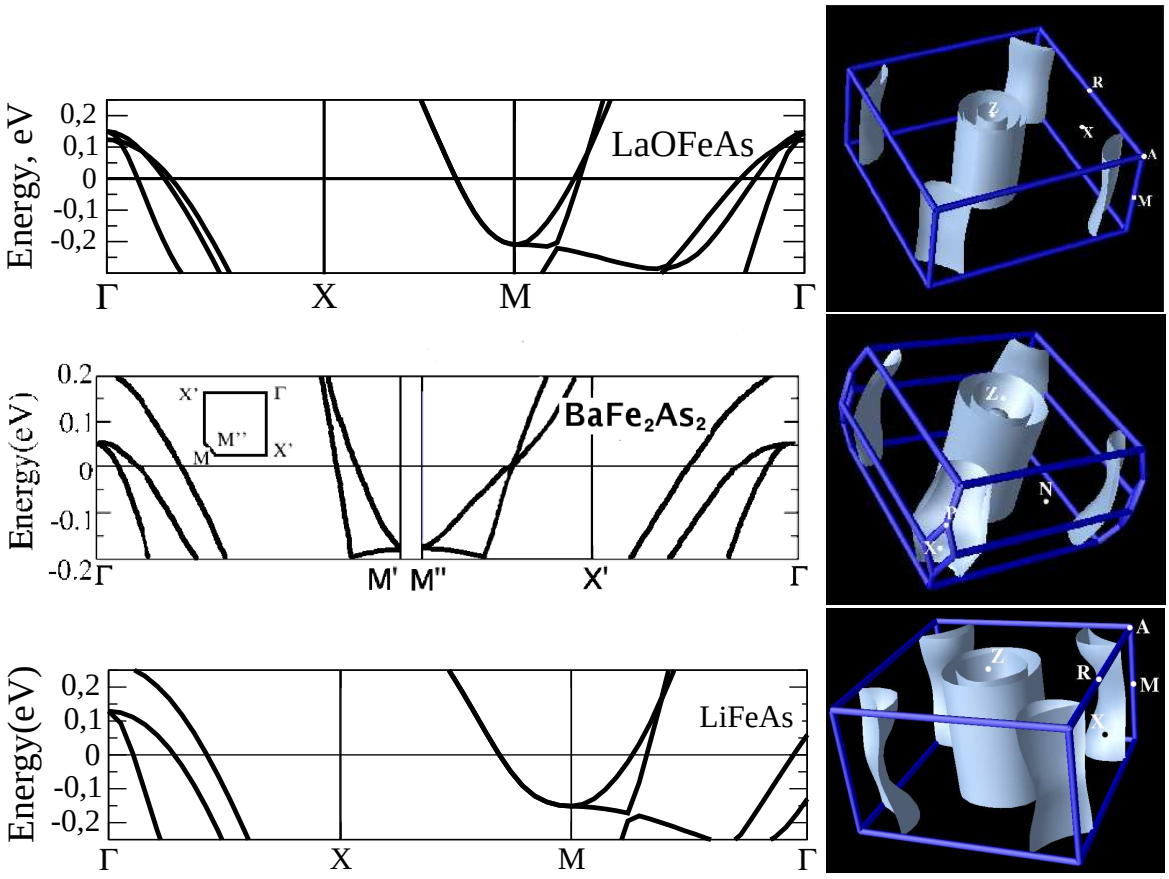

FIG. 21: Left – electronic spectrum of $LaO_{1-x}F_xFeAs$, $BaFe_2As_2$ and $LiFeAs$ in a narrow interval of energies close to the Fermi level, relevant to the formation of superconducting state. Right – Fermi surfaces of these compounds [117, 119].

and the values of T_c in these compounds).

The bandwidth of d-states of Fe in $BaFe_2As_2$ is approximately 0.3 eV larger than in LaOFeAs, which may be connected with shorter Fe-As bonds, i.e. with larger Fe-d-As-p hybridization. In both compounds bands crossing the Fermi level are formed mainly from three d-orbitals of Fe with t_{2g} symmetry – xz, yz, xy. Similar situation is realized also in case of $LiFeAs$.

In Fig. 21 (left) we show electronic dispersions in high symmetry directions in all three main classes of new superconductors (1111, 122 111) in a narrow ($\pm$ 0.2 eV) energy interval around the Fermi level, where superconducting state is formed [118, 119]. It can be seen that electronic spectra of all systems in this energy interval are very close to each other. In general case, the Fermi level is crossed by five bands, formed by d-states of Fe. Of these, three form hole – like Fermi surface pockets close to Γ – point, and the other two – electron – like pockets at the corners of Brillouin zone (note that Brillouin zones of 1111, 111 and 122 systems are slightly different due to differences in lattice symmetry).

It is clear that this kind of a band structure leads to similar Fermi surfaces of these compounds — appropriate calculation results are shown in the right side of Fig. 21: there are three hole–like cylinders at the center of Brillouin zone and two electron – like at the corners. Almost cylindrical form of the Fermi surface reflects quasi two – dimensional nature of electronic spectrum in new superconductors. The smallest of hole – like cylinders is usually neglected in the analysis of superconducting pairings, as its contribution to electronic properties is rather small (smallness of its phase space volume). At the same time, from the general picture of electronic spectrum it is clear that superconductivity is formed in multiple band system with several Fermi surfaces of different (electron or hole – like) nature, which is drastically different from the simple one – band situation in cuprates. Below we shall see that results of LDA calculations of electronic structure correlate rather well with experiments on angle resolved photoemission (ARPES).

LDA calculations of band structure of α-FeSe were performed in a recent paper [116]. Dropping the details we note that the results are qualitatively quite similar to those described above for 1111, 122 and 111 systems. In particular, the form of Fermi surfaces is qualitatively the same, while conduction bands near the Fermi level are formed from

d-states of Fe.

First calculations of band structure of Sa(Ca)FFeAs compounds were done in Refs. [120, 121]. Naturally enough, the band structure and Fermi surfaces in these compounds are also very similar to those obtained before for REOFeAs systems. The only difference is slightly more pronounced quasi two – dimensional nature of the spectra in these compounds.

"Minimal" model

Relative simplicity of electronic spectrum of FeAs superconductors close to the Fermi level (Fig. 21) suggests a possibility to formulate a kind of "minimal" analytic or semi – analytic model of the spectrum (e.g. in the tight – binding approximation), which will provide semi – quantitative description of electrons in the vicinity of the Fermi level, sufficient for theoretical description of superconducting state and magnetic properties of FeAs planes. Up to now several variants of such model were already proposed [127, 128, 129, 130]. Below we shall limit ourselves to brief description of the simplest (and most crude) variant of such model proposed by Scalapino et al. [127].

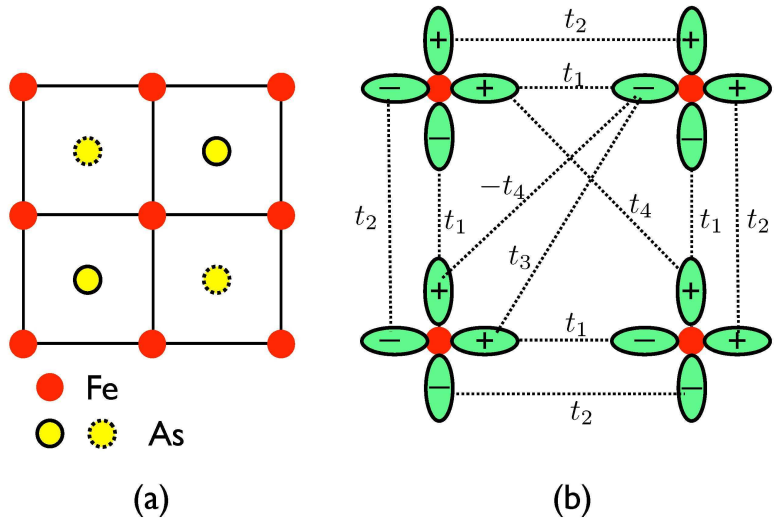

FIG. 22: (a) Fe ions in FeAs layer form quadratic lattice, containing two Fe ions and two As ions in elementary cell. As ions are placed above (filled circles) or under (dashed circles) centers of the squares formed by Fe, (b) transfer integrals taken into account in two – orbital (d_{xz}, d_{yz}) model on the square lattice of Fe. Here t_1 – transfer integral between nearest σ-orbitals, and t_2 – transfer integral between nearest π-orbitals. Also taken into account are transfer integrals t_4 between different orbitals and t_3 between identical orbitals on the second nearest neighbors. Shown are projections of d_{xz}, d_{yz} orbitals on xy plane [127].

Schematic structure of a single FeAs layer is shown in Fig. 22 (a). Fe ions form the square lattice, surrounded by As layers, which also form the square lattice and are placed in the centers of squares of Fe ions and are displaced upwards or downwards with respect to Fe lattice in a checkerboard order, as shown in Fig. 22 (a). This leads to two inequivalent positions of Fe, so that there are two ions of Fe and two As ions in an elementary cell. LDA calculations described in the previous section show that the main contribution to electronic density of states in a wide enough energy interval around the Fermi level as due to d - states of Fe. Thus, we can consider the simplified model which primarily takes into account three orbitals of Fe, i.e. d_{xz}, d_{yz} and d_{xy} (or $d_{x^2-y^2}$, which is just the same). As a further simplification the role of d_{xy} (or $d_{x^2-y^2}$) orbitals can be effectively taken into account introducing transfer integrals between d_{xz}, d_{zy} orbitals on the second nearest neighbors. Accordingly, we may consider the square lattice with two degenerate "d_{xz}, d_{yz}" orbitals at each site, with transfer integrals shown in Fig. 22 (b). As we shall see below, such model produces the picture of two – dimensional Fermi surfaces of FeAs layer, which is in qualitative agreement with LDA results.

For analytical description of this model it is convenient to introduce a two – component spinor

$$\psi_{\mathbf{k}s} = \begin{pmatrix} d_{xs}(\mathbf{k}) \\ d_{ys}(\mathbf{k}) \end{pmatrix} \tag{2}$$

where $d_{xs}(\mathbf{k})$ ($d_{ys}(\mathbf{k})$) annihilates d_{xz} (d_{yz}) electron with spin s and wave vector $\mathbf{k}$. Tight – binding Hamiltonian can be written as

$$H_0 = \sum_{\mathbf{k}s} \psi^+_{\mathbf{k}s} \left[\left(\varepsilon_+(\mathbf{k}) - \mu \right) 1 + \varepsilon_-(\mathbf{k}) \tau_3 + \varepsilon_{xy}(\mathbf{k}) \tau_1 \right] \psi_{\mathbf{k}s}, \tag{3}$$

where τ_i are Pauli matrices,

$$\begin{aligned}
\varepsilon_\pm(\mathbf{k}) &= \frac{\varepsilon_x(\mathbf{k}) \pm \varepsilon_y(\mathbf{k})}{2}, \\
\varepsilon_x(\mathbf{k}) &= -2t_1 \cos k_x a - 2t_2 \cos k_y a - 4t_3 \cos k_x a \cos k_y a, \\
\varepsilon_y(\mathbf{k}) &= -2t_2 \cos k_x a - 2t_1 \cos k_y a - 4t_3 \cos k_x a \cos k_y a, \\
\varepsilon_{xy}(\mathbf{k}) &= -4t_4 \sin k_x a \sin k_y a.
\end{aligned}$$

Finally, the single – particle Green's function in Matsubara representation takes the following form

$$\hat{G}_s(\mathbf{k}, i\omega_n) = \frac{\left(i\omega_n - \epsilon_+(\mathbf{k}) \right) \hat{1} - \epsilon_-(\mathbf{k}) \hat{\tau}_3 - \epsilon_{xy}(\mathbf{k}) \hat{\tau}_1}{\left(i\omega_n - E_+(\mathbf{k}) \right) \left(i\omega_n - E_-(\mathbf{k}) \right)} \tag{4}$$

where

$$E_\pm(\mathbf{k}) = \epsilon_+(\mathbf{k}) \pm \sqrt{\epsilon^2_-(\mathbf{k}) + \epsilon^2_{xy}(\mathbf{k})} - \mu \tag{5}$$

In Fig. 23 (a) we show the appropriate electronic spectrum for the values of transfer integrals $t_1 = -1, t_2 = 1.3, t_3 = t_4 = -0.85$ (in units of $|t_1|$).

Now take into account the fact, mentioned above, that in real FeAs layer there are two Fe ions per elementary cell. Accordingly, the Brillouin zone is twice smaller and the spectrum must be folded down into this new zone as shown in Fig. 23 (b). In Fig. 23 (c,d) we show Fermi surfaces, which are obtained in this simplified model of electronic spectrum. In large Brillouin zone, corresponding to the lattice with one Fe ion per elementary cell, there are two hole – like pockets, denoted as α_1 and α_2, which are defined by the equation $E_-(k) = 0$, and two electron – like pockets β_1 and, defined by $E_+(k) = 0$. To compare with the results of band structure calculations (LDA) these Fermi surfaces should be folded down to twice smaller Brillouin zone, corresponding to two Fe ions in elementary cell of the crystal, which is shown by dashed lines in Fig. 23 (c). The result of such downfolding is shown in Fig. 23 (d). We can see that the Fermi surfaces obtained in this way are in qualitative agreement with the results of LDA calculations (only the third, less relevant, small hole – like pocket in the zone center is absent). Despite its crudeness this model of the spectrum, proposed in Ref. [127], is quite appropriate for qualitative analysis of electronic properties of FeAs superconductors.

Angle resolved photoemission spectroscopy (ARPES)

At the moment there are already a number of papers, where electronic spectrum and Fermi surfaces in new superconductors were studied using angle resolved photoemission spectroscopy (ARPES) [131, 132, 133, 134, 135, 136, 137, 138, 139, 140, 141], reliable method, which proved its effectiveness in HTSC – cuprates [13, 142], due by the way to quasi two – dimensional nature of electronic spectrum in these systems. In fact, for FeAs superconductors ARPES studies immediately provided valuable information clarifying the general form of the spectrum, Fermi surfaces and the values and peculiarities of superconducting gaps. Note that for 1111 systems up to now there is only one ARPES work [131], which is due to the absence of good single crystals, so that all the remaining studies were performed on single crystals of 122 systems. Below we shall discuss the results of some of these papers in more details.

ARPES measurements in Ref. [131] were performed on a single crystal of micron sizes (of the order of 200×200×30 μm, with $T_c \sim 53$K). In Fig. 24 we show ARPES intensity maps (which is proportional to spectral density) in $NdO_{0.9}F_{0.1}FeAs$ system, allowing to determine the form of Fermi surfaces in two – dimensional Brillouin zone, corresponding to FeAs planes. It can be seen that the general qualitative picture is in reasonable agreement with the results of LDA calculations of the band structure, though around the Γ point only one hole – like cylinder is resolved, and electron – like cylinders in the corners (point M) are resolved rather poorly. The value of superconducting gap on the hole – like cylinder estimated from ARPES spectra was determined to be of the order of 20 meV [131], corresponding to $2\Delta/T_c \sim 8$.

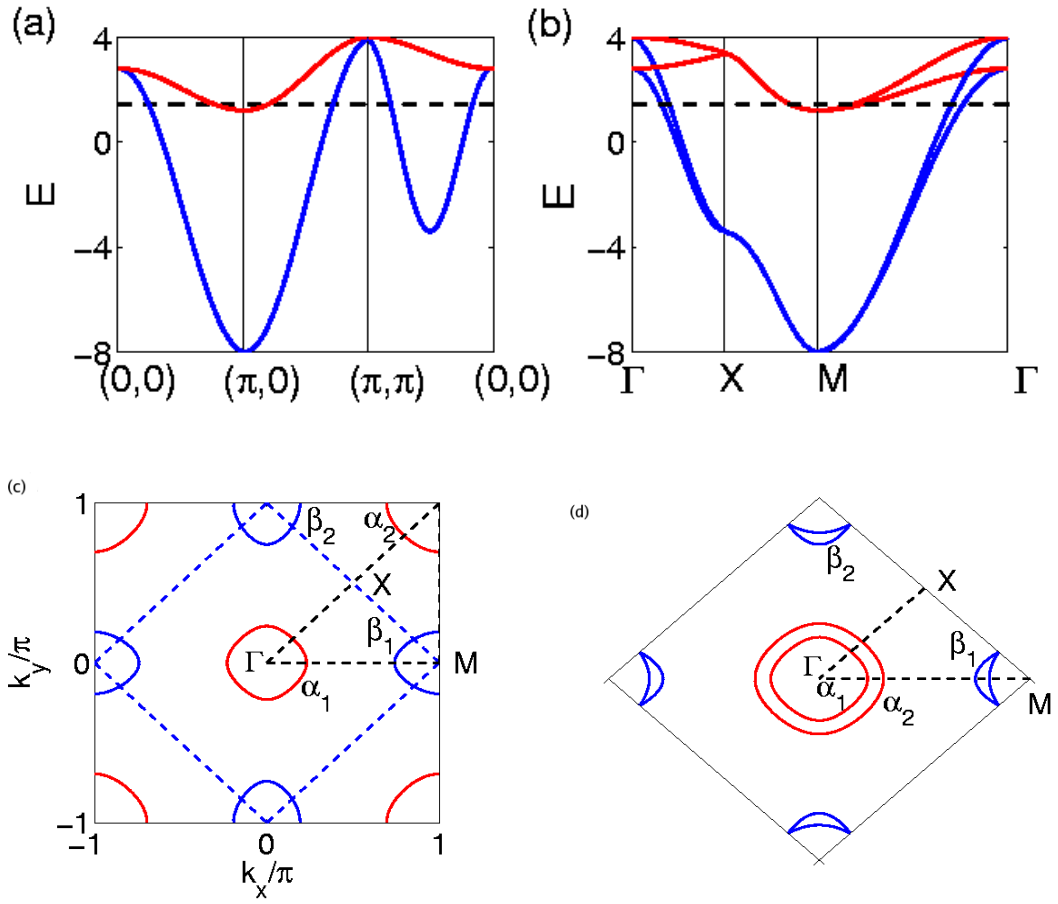

FIG. 23: (a) electronic spectrum in two – orbital model with transfer integrals $t_1 = -1, t_2 = 1.3, t_3 = t_4 = -0.85$ (in units of $|t_1|$) and chemical potential $\mu = 1.45$, along directions $(0,0) \to (\pi/a, 0) \to (\pi/a, \pi/a) \to (0,0)$, (b) the same spectrum in downfolded Brillouin zone, with appropriate redefinition of Γ, X, M points, (c) Fermi surface in two – orbital model in the Brillouin zone, corresponding to one Fe ion per elementary cell. $\alpha_{1,2}$ – hole – like Fermi surfaces, defined by $E_-(k_F) = 0$, $\beta_{1,2}$ – electron – like Fermi surfaces, defined by $E_+(k_F) = 0$. Dashed lines show the Brillouin zone for the case of two Fe ions in elementary cell, (d) Fermi surfaces in downfolded Brillouin zone, corresponding to two Fe ions in elementary cell [127].

In Ref. [134] ARPES measurements were performed on a single crystal of superconducting (Sr,K)Fe_2As_2 with $T_c = 21$K. ARPES map of the Fermi surfaces obtained is shown in Fig. 25. In contrast to other works, here the authors succeeded in resolving all three hole – like cylinders around the point Γ, in complete agreement with majority of LDA calculations of the spectrum. Resolution in the corners of Brillouin zone (point M) was much poorer, so that the topology of electronic sheets of the Fermi surface remained unclear.

In Fig. 26 we show energy bands in high symmetry directions of Brillouin zone obtained from ARPES measurements [134]. First of all, these data correlate well with the results of band structure calculations of Ref. [118], with the account of Fermi level shift downwards in energy by ~ 0.2 eV (in complete accordance with hole doping of superconducting sample). On the other hand, rather significant band narrowing in comparison with LDA results is also observed, which can be attributed to strong electronic correlations (cf. below).

In Ref. [136] for the first time were studied in detail not only Fermi surfaces of $Ba_{0.6}K_{0.4}Fe_2As_2$ ($T_c = 37$K) [5], but also ARPES measurements were done of superconducting gaps (and their temperature dependence) on different sheets of the Fermi surface. Schematically, results of these measurements are shown in Fig. 27. Two superconducting gaps were discovered – a large one ($\Delta \sim 12$ meV) on small hole – like cylinder around point Γ and also on electron –

[5] The third small hole – like cylinder around point Γ was not observed, probably due to insufficient resolution of ARPES spectra.

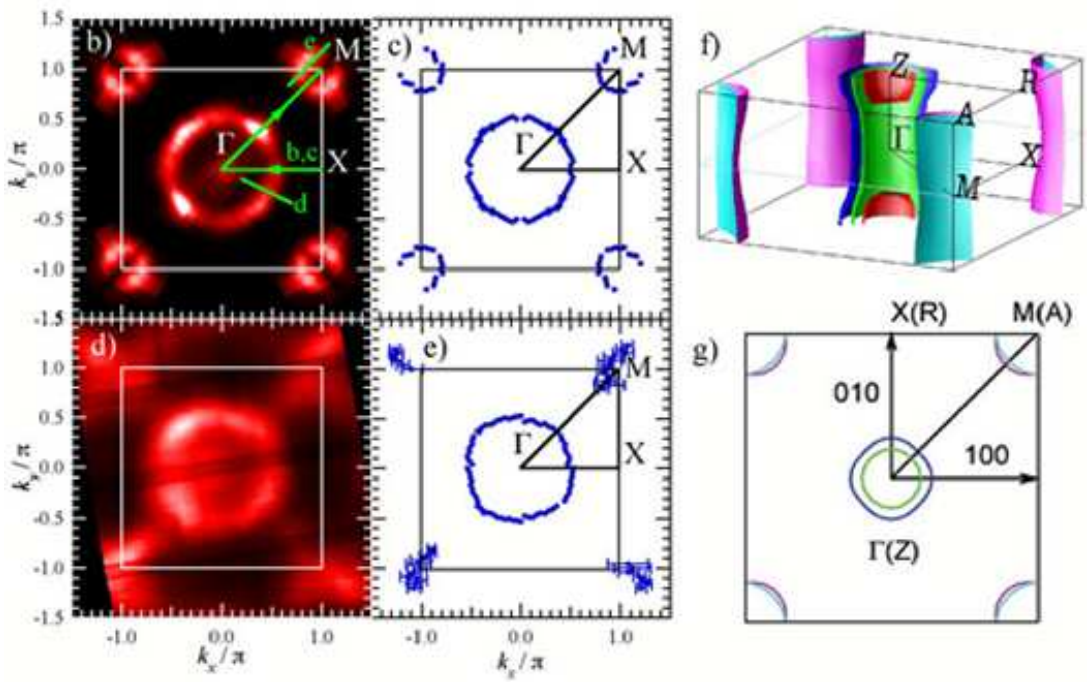

FIG. 24: (b) ARPES intensity map and (c) Fermi surfaces determined for $NdO_{0.9}F_{0.1}FeAs$, at photon energy 22 eV and $T = 70$K, (d,e) – the same, but for photon energy 77 eV [131], (f,g) three – dimensional two – dimensional picture of Fermi surfaces in NdOFeAs, obtained from LDA calculations [131].

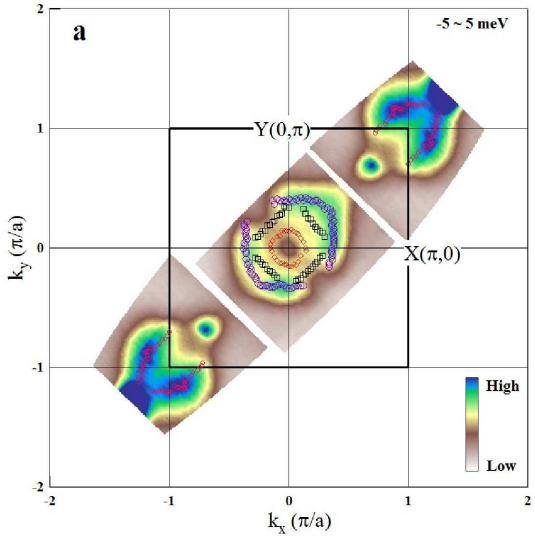

FIG. 25: ARPES map of Fermi surfaces in $(Sr, K)Fe_2As_2$ [134].

like cylinders around point M, and a small one ($\Delta \sim 6$ meV) on big hole – like cylinder around Γ point. Both gaps close at the same temperature coinciding with T_c, have no zeroes and are practically isotropic on appropriate sheets of the Fermi surface. Accordingly, $2\Delta/T_c$ ratio is different on different sheets (cylinders) and formally are consistent with both strong (large gap, the ratio is 7.5) and weak (small gap, the ratio is 3.7) coupling. These results correspond to the picture of generalized s - wave pairing, to be discussed below.

Quite similar results on gap values on different sheets of the Fermi surface were obtained also in Ref. [137] via ARPES measurements on single crystals of $(Sr/Ba)_{1-x}K_xFe_2As_2$. Also in this work the electron dispersion was measured by ARPES in rather wide energy interval, which demonstrated characteristic "kinks", attributed to conduction electrons interaction with collective oscillations (phonons or spin excitations), allowing determination of electron velocity close

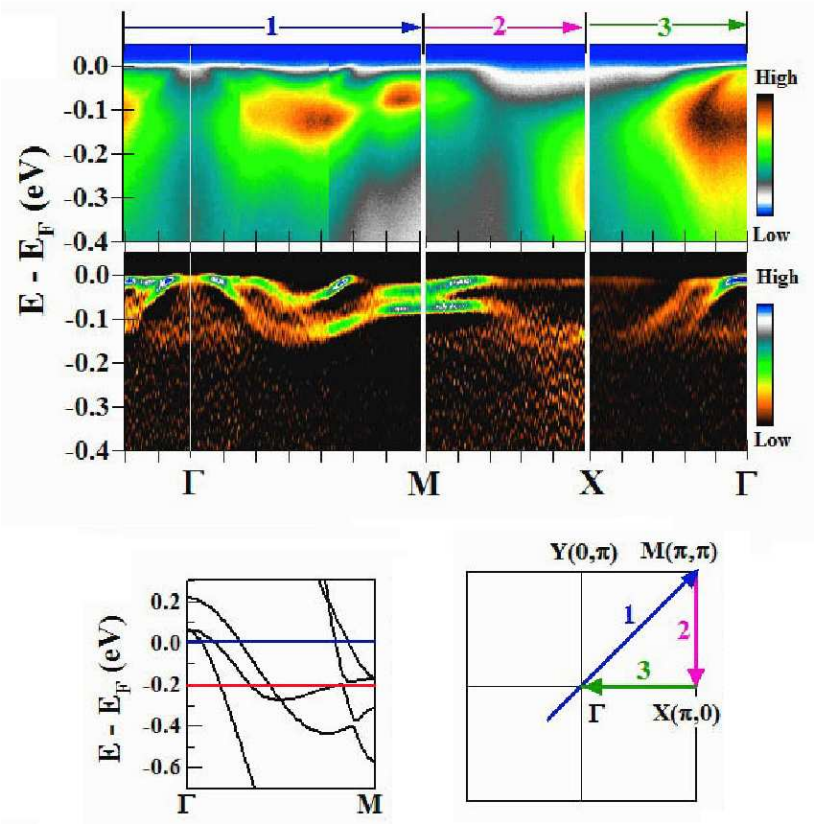

FIG. 26: Energy bands determined from ARPES data in $(Sr, K)Fe_2As_2$[134], in upper part of the figure – raw ARPES data, below – their second derivative, allowing to follow dispersion curves. Below to the left – band spectrum obtained in Ref. [118], and to the right – directions in the Brillouin zone, along which measurements have been made.

to the Fermi level: $v_F \sim 0.7 \pm 0.1$ eV Å, so that using the value of the "large" gap $\Delta \sim 12 \pm 2$ meV gives an estimate of coherence length (the size of Cooper pairs) $\xi_0 = \frac{\hbar v_F}{\Delta} < 20$ Å, i.e. relatively small value (compact pairs).

Rather unexpected results for the topology of Fermi surfaces were obtained in Refs. [139, 140] for $Ba_{1-x}K_xFe_2As_2$, where Fermi surface sheets close to the M point were discovered to have a characteristic "propeller" – like form, which does not agree with any LDA calculations. Measurements of superconducting gap in Ref. [140] has given for the "large" gap on an "internal" hole – like cylinder around Γ point the value of $\Delta \sim 9$ meV and the same value on "propellers" close to M points, which corresponds to the value of $2\Delta/T_c = 6.8$. On an "external" hole – like cylinder around point Γ the value $\Delta < 4$ meV was obtained, corresponding to $2\Delta/T_c < 3$.

Note also Ref. [141], where ARPES measurements were performed on "maximally doped" variant of $Ba_{1-x}K_xFe_2As_2$ system with $x = 1$, i.e. on superconducting KFe_2As_2 ($T_c = 3$K). It was discovered that the form of hole – like Fermi surfaces (sheets) surrounding Γ point is qualitatively the same as in $Ba_{1-x}K_xFe_2As_2$ with $x = 0.4$ (T_c=37K), while electron – like cylinders surrounding M points are just absent. This is a natural consequence of the downward shift of the Fermi level due to hole doping (cf. Fig. 21, where it is clearly seen that electronic branches of the spectrum are above the Fermi level in case of its big enough downward energy shift). Besides that, similarly to Ref. [134], the observed bands are significantly (2-4 times) narrower, than obtained in all LDA – type calculations. This fact, as already noted above, is most probably due to strong enough electronic correlations (see next section). The absence of electronic pockets of the Fermi surface leads to the disappearance of interband mechanisms of pairing (see below) and corresponding significant lowering of T_c.

Summing up, it can be noted that the results of ARPES studies of Fermi surfaces and electronic spectrum of FeAs superconductors are in rather satisfactory with LDA calculations of band structure. Remaining inconsistencies are most probably due to unaccounted role of electronic correlations and, sometimes, due to insufficient resolution in ARPES experiments.

Unfortunately, up to now there are almost no experiments on determination of Fermi surfaces from low temperature quantum oscillations (like de Haas – van Alfen). We can only note Ref. [143], where non superconducting phase of

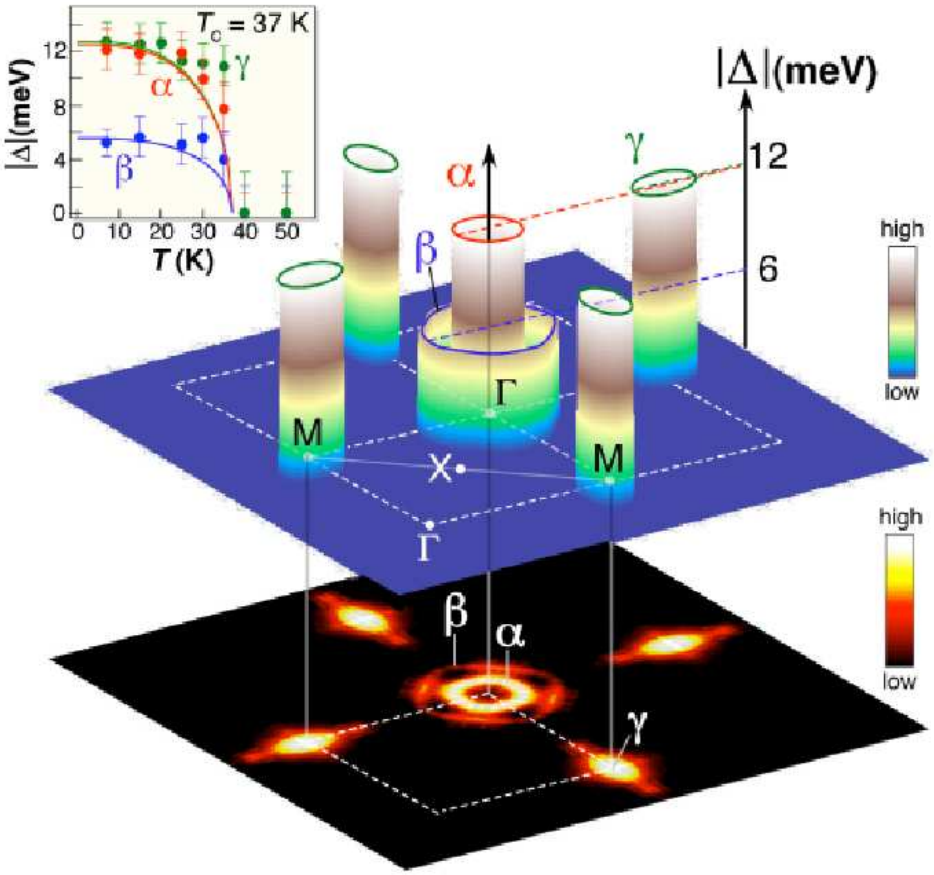

FIG. 27: Schematic three – dimensional picture of superconducting gap in $Ba_{0.6}K_{0.4}Fe_2As_2$ according to ARPES measurements [136]. Below – Fermi surfaces (ARPES intensity), at the insert above – temperature dependences of gaps on different sheets of the Fermi surface.

$SrFe_2As_2$ was studied and oscillation periods discovered corresponded to small Fermi surface pockets, which apparently can be attributed to hole – like cylinders close to Γ point, almost completely "closed" by antiferromagnetic gap. In Ref. [144] quantum oscillations were studied in LaOFeP and found to be in agreement with Fermi surface predicted by LDA calculations, with additional two times mass enhancement.

Correlations (LDA+DMFT)

LDA calculations of electronic spectrum neglect potentially strong effects of local electron correlations (Hubbard – like repulsion of electrons), which can be naturally expected in bands, formed mainly from *d*-states of Fe in FeAs layers. Most consistent approach to the analysis of such correlations at present is considered to be the dynamical mean field theory (DMFT) [145, 146, 147, 148, 149], including its variant taking into account the LDA band structure of real systems (LDA+DMFT) [150, 151, 152].

LDA+DMFT approach was used to calculate electronic structure of FeAs compounds in Refs. [153, 154, 157, 158, 159]. In all of these, except Ref. [158], only LaOFeAs system was studied, while in Ref. [158] the authors analyzed the series of REOFeAs (RE=La,Ce,Pr,Nd).

In Ref. [153] LDA+DMFT was used to calculate spectral density and optical conductivity of $LaO_{1-x}F_xFeAs$. The value of Hubbard repulsion was taken to be U =4 eV, while Hund (exchange) coupling was assumed to be

equal to J =0.7 eV [6]. In Fig. 28 we show the results for momentum dependence of the spectral density in high symmetry directions in the Brillouin zone. Position of the maxima of spectral density describe the effective dispersion of (damped) quasiparticles, which may be compared with results of LDA calculations (infinite lifetime quasiparticles), which are also show. Doping was described in virtual crystal approximation. It can be seen that electron correlations lead to a significant (3-5 times) enhancement of effective masses and strong damping of quasiparticles. System remains metallic, though a kind of a "bad" metal with strongly renormalized quasiparticle amplitude (residue at the Green's function pole) $Z \sim 0.2 - 0.3$.

The general picture of the spectrum shown in Fig. 28 can be qualitatively compared with ARPES data, shown in the lower part of Fig. 26. Though the experiment was done on another system certain similarity is obvious — conduction bands are significantly narrowed (in comparison with LDA results), while in the energy region around -0.5 eV the bands are just "destroyed" and there a kind of energy gap there.

According to Ref. [153] even rather small enhancement of Hubbard repulsion up to U =4.5 eV makes transforms this system into a kind of Mott insulator with an energy gap at the Fermi level. Thus it was concluded that systems under consideration are characterized by intermediate correlations and are close to Mott insulator, making them partly similar to HTSC cuprates. At the same time, contrary to cuprates, prototype (undoped) compounds are metals, not Mott insulators.

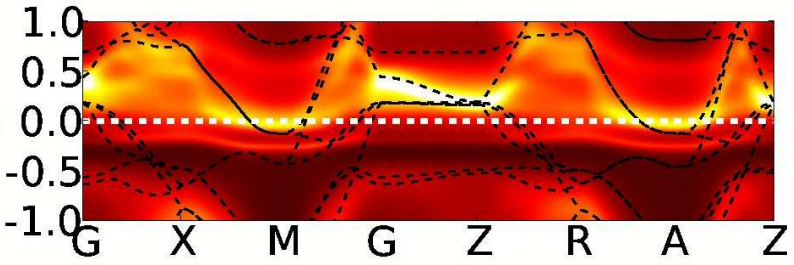

FIG. 28: Momentum dependence of spectral density (positions of the maxima of define effective dispersion of quasiparticles) in LDA+DMFT approximation for LaOFeAs with 10% doping. Dashed lines – results of LDA approximation [153].

Quite different conclusion was reached by the authors of Ref. [154], which performed formally the same type of calculations (by the same methods and with the same choice of parameters). In this work it was claimed that even the use of U values up to U 5 eV does not transform a system into Mott insulator and changes in spectral density (electron dispersion) and density of states due to correlations are rather insignificant.

At present the reasons for such drastic differences of results obtained by two leading groups making LDA+DMFT calculations are unclear.

In general it should be noted that "ab initio" nature of LDA+DMFT approach is rather relative, as e.g. the value of Hubbard interaction U is, in fact, a kind of (semi)phenomenological parameter. There exists a number of "ab initio" approaches to calculate its value, of which most consistent is assumed to be the so called method of constrained random phase approximation (constrained RPA) [155, 156]. Within this approach the value of local Hubbard repulsion is calculated from the "bare" Coulomb repulsion V using the RPA expression:

$$U = \frac{V}{1 - V\Pi_r} \tag{6}$$

where Π_r is polarization operator, taking into account screening by electrons from the outside of (correlated) bands of interest. For example, if we limit ourselves only to the analysis of bands formed by d-states of Fe, we have to use $\Pi_r = \Pi - \Pi_d$, where Π_d is polarization operator calculated only on d-states. It is clear that the value of U defined in this way depends on the assumed scheme of calculations (the account of different groups of screening electrons).

For FeAs compounds this problem was studied in Ref. [158]. The values of different interaction parameters entering to LDA+DMFT calculation scheme, obtained by exclusion of different groups of states from screening of the "bare" Coulomb interaction, are given in Table IV.

[6] DMFT impurity problem was solved by quantum Monte Carlo (QMC) with temperature taken to be 116 K.

Table IV. "Bare" and partly screened Coulomb interactions V and U, and Hund coupling J for LaOFeAs, obtained in Ref. [158] by exclusion different groups of states (listed in the first column) from screening.

	V (eV)	U (eV)	J (eV)
d	15.99	2.92	0.43
dpp	20.31	4.83	0.61
d-dpp	20.31	3.69	0.58

We can see that the values of interaction parameters, entering LDA+DMFT scheme, can change in rather wide intervals.

The same questions were discussed in Refs. [157, 159] (within constrained DFT approach [160]), with authors coming to the conclusion that effective parameters of Coulomb (Hubbard) repulsion are relatively small, if we limit ourselves within the basis of *d*-states of Fe. Accordingly, LDA+DMFT calculations, performed in these works, produced electronic structure, which is only slightly different from LDA results.

In the opinion of authors of Refs. [154, 157, 159], their conclusion about the smallness of electronic correlations in FeAs systems is confirmed by experiments on X-Ray absorption qnd emission spectroscopy of Ref. [161], however it is in sharp contrast with ARPES data [134, 141], which definitely indicate rather strong renormalization of electronic spectrum due to correlations. It should be stressed that data on the topology of Fermi surfaces are, in fact, insufficient to make any judgements on the role of correlations — Fermi surfaces in LDA+DMFT approach are just the same as in LDA approximation. It is important to study in detail electronic dispersion, bandwidths and quasiparticle damping far enough from the Fermi level, as well as quasiparticle residue Z. In our opinion, ARPES measurements have many advantages here and can help to solve this important problem.

Summarizing, the question of the role of electronic correlations in new superconductors is still under discussion. It is most probable that correlations in these systems are of intermediate strength between typical metals and systems like Mott insulators, so that we are dealing here with the state of *correlated* metal [147, 149].

Spin ordering: localized or itinerant spins?

In this section we shall briefly consider theoretical ideas on the nature of antiferromagnetic ordering in undoped FeAs compounds and closely related problem of structural transition from tetragonal to orthorhombic phase. Strictly speaking, these questions are slightly outside the scope of our review (superconductivity in FeAs compounds), so that our presentation will be very short.

Possibility of antiferromagnetic ordering in systems under consideration was noted even before direct neutronographic observations discussed above. Already in one of the earliest papers on electronic structure of iron oxypnictides [110], as well as during the analysis of "minimal" two – band model [127], it was stressed that there is an approximate "nesting" of hole – like Fermi surfaces around Γ point and electron – like Fermi surfaces around M point. It is most easily seen e.g. in Fig. 23 (c) — the shift of hole – like cylinder by vector $(\pi, 0)$ or $(0, \pi)$ leads to its approximate coincidence with electron – like cylinder. Direct calculations show [110, 127] that this fact leads to formation of rather wide, but still quite noticeable, peak in static magnetic susceptibility $\chi_0(\mathbf{q})$ (determined by appropriate loop diagram) at $\mathbf{q} = (\pi, 0)$ and $\mathbf{q} = (0, \pi)$. In its turn, this may lead to antiferromagnetic instability towards formation of spin density wave (SDW) with appropriate wave vector, at least in case of strong enough exchange interaction. Above we have seen that precisely this type of spin ordering is observed experimentally in FeAs layers [69, 71, 74, 76, 77, 78]. Also observed rather small values of magnetic moments on Fe also give an evidence for the itinerant nature of magnetism (SDW). It is also natural to assume that in doped (superconducting) compounds well developed spin fluctuation of SDW type persist, giving a way to pairing interaction of electrons.

At the same time, magnetic ordering in FeAs layers can be analyzed also within more traditional approach, based on the qualitative picture of localized spins on Fe ions, interacting via the usual Heisenberg exchange between nearest and second nearest neighbors. Such analysis was performed e.g. in Ref. [162] for LaOFeAs, as well as "ab initio" calculations of appropriate exchange integrals and values of magnetic moments. For us more important are qualitative aspects of this analysis, which are illustrated by Fig. 29 [162].

In this figure we show two possible antiferromagnetic configurations of spins in FeAs layer. In the experiments [69] the AF2 (see Fig. 29) type spin structure is observed, which is realized when inequality $J_1 < 2J_2$ holds, where J_1 is an exchange integral between nearest, and J_2 – between second nearest neighbors, with both integrals assumed positive (antiferromagnetism). Direct (FP-LAPW) calculation of ground state energy of LaOFeAs, performed in

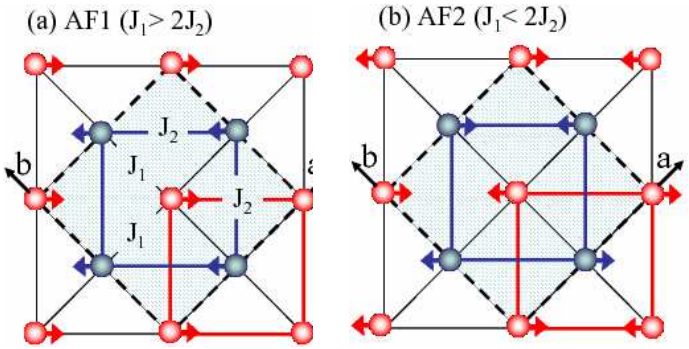

FIG. 29: Two alternative spin configurations in antiferromagnetic FeAs layer: (a) – antiparallel spins on nearest neighbors, (b) – antiparallel spins on on second nearest neighbors [162].

Ref. [162], confirmed the greater stability of this state. AF2 configuration can be considered as two interpenetrating antiferromagnetic square sublattices, shown by different colors in Fig. 29. In this case each Fe ion is placed in the center of antiferromagnetically ordered call, so that the mean molecular field on its spin is just zero. In this case each sublattice may freely (with no cost in energy) rotate with respect to the other. This is a situation of complete frustration. It is well known that such a state is usually unstable with respect to structural distortions. Thus, it can be expected that a structural distortion will appear in our system, making spins at a pair of Fe ions closer to each other, while the pair on the other side of a square slightly farther apart. This is just the type of distortion (tetra – ortho transition) observed in the experiment [69]. Direct calculations of total energy confirm this guess [162].

However, the general situation with the nature of magnetic ordering and structural transition in FeAs layers is rather far from being completely clear. "Ab initio" calculations as a rule produce strongly overestimated values of magnetic moments of Fe, while the relative stability of magnetic structures strongly depends on details of methods used. Apparently, this is due to the itinerant nature of magnetism in these systems. Detailed discussion of these problems can be found in interesting papers [163, 164], where an original qualitative picture of strong magnetic fluctuations is proposed, allowing, in the authors opinion, to explain all the anomalies of magnetic properties.

MECHANISMS AND TYPES OF PAIRING

After the discovery of high – temperature superconductivity in iron based layered compounds a dozens of theoretical papers appeared with different proposals on possible microscopic mechanisms and types of Cooper pairing in these systems. The review of all these papers here seems impossible and below we shall deal only with very few, in our opinion, most important works.

Multi – band superconductivity

Main peculiarity of new superconductors is their multiple – band nature. Electronic structure in a narrow enough energy interval around the Fermi level is formed practically only from *d*-states of Fe. Fermi surface consists of several hole – like and electron – like cylinders and on each its "own" energy gap can be formed. From the general point of view this situation is not new and was already analyzed in the literature [165]. However, for the case of specific band structure typical for FeAs layers we need an additional analysis.

In general enough formulation this problem was considered in a paper by Barzykin and Gor'kov [166] and some of the results will be presented below. Typical electronic spectrum of FeAs layered systems in the relevant (for superconductivity) energy interval was shown in Fig. 21. Similar, in principle, spectrum was obtained also in the "minimal" model of Ref. [127]. An oversimplified view of this spectrum is shown in Fig. 30 [166].

This form of Fermi surfaces corresponds to stoichiometric (undoped) composition of these compounds, and electrons and holes occupy the same volumes (compensated semi – metal)[7] Electronic doping shrinks hole – like pockets, while

[7] In fact, just this form of the spectrum was assumed in numerous papers on excitonic instability and excitonic insulator [167, 168, 169,

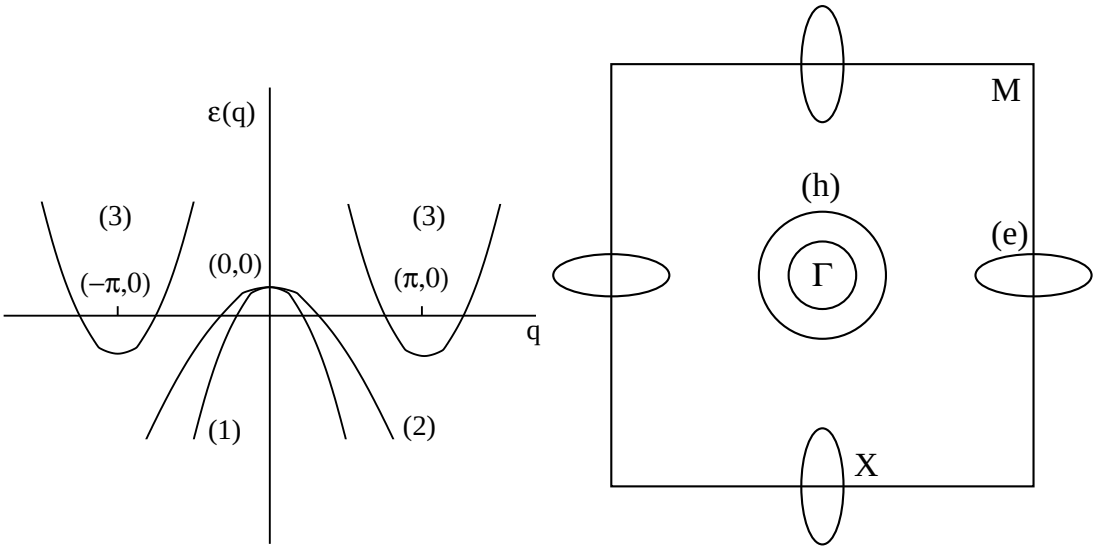

FIG. 30: Schematic view of electronic spectrum (a) and Fermi surfaces for LaOFeAs in extended band picture. Around point Γ there are two hole – like sheets, while electron – like sheets are around X points [166].

hole doping — electron – like pockets.

In Ref. [166] a symmetry analysis of possible types of superconducting order parameter was performed, along the lines of Refs. [172, 173], and also the explicit solutions of BCS equations were found for the system with electronic spectrum shown in Fig. 30 .

Let $\Delta_i(p)$ be a superconducting order parameter (gap) on the i-th sheet of the Fermi surface. The value of $\Delta_i(\mathbf{p})$ is determined by self – consistency equation for the anomalous Gor'kov's function $F_i(\omega_n, \mathbf{p})$:

$$\Delta_i(\mathbf{p}) = T \sum_{j;\omega_n} \int V^{i,j}(\mathbf{p} - \underline{\mathrm{p}}')d\mathbf{p}' F_j(\omega_n, \mathbf{p}') \tag{7}$$

where $V^{i,j}(\mathbf{p} - \mathbf{p}')$ is the pairing interaction. If Fermi surface pockets are sufficiently small (as it seems to be in FeAs systems), transferred momentum $\mathbf{p} - \mathbf{p}'$ within each pockets is also small and we can replace $V^{i,j}(\mathbf{p} - \mathbf{p}')$ by $V^{i,j}(0)$, which is favorable for the formation of momentum independent gaps.

Pairing BCS interaction in this model can be represented by the following matrix:

$$V = \begin{pmatrix} u & u & t & t \\ u & u & t & t \\ t & t & \lambda & \mu \\ t & t & \mu & \lambda \end{pmatrix}. \tag{8}$$

where $\lambda = V^{eX,eX} = V^{eY,eY}$ defines interaction on an electron – like pockets at point X, $\mu = V^{eX,eY}$ connects electrons from different pockets at points $(\pi, 0)$ and $(0, \pi)$, $u = V^{h1,h1} = V^{h2,h2} = V^{h1,h2}$ characterizes BCS interaction on two hole – like pockets[8], surrounding the point Γ, while $t = V^{h,eX} = V^{h,eY}$ connects electrons from points X and Γ.

Critical temperature of superconducting transition T_c is determined by the solution of the system of linearized gap equations:

$$\Delta_i = \sum_j \bar{V}^{i,j} \Delta_j \ln \frac{2\gamma\bar{\omega}}{\pi T_c}, \tag{9}$$

170, 171]. This instability may be considered as an alternative explanation of antiferromagnetic ordering and structural transition in these systems [166].

[8] An assumption that these couplings are the same seems to us to be too rigid.

where $\bar{\omega}$ is the usual cut – off frequency of logarithmic divergence in Cooper channel, and

$$\bar{V}^{i,j} \equiv -\frac{1}{2} V^{i,j} \nu_j, \tag{10}$$

where ν_j is the density of states on the j-th sheet (pocket) of the Fermi surface.

Introducing an effective coupling constant g and writing down T_c as:

$$T_c = \frac{2\gamma\bar{\omega}}{\pi} e^{-2/g}, \tag{11}$$

we obtain solutions of three types:

1) solution corresponding to $d_{x^2-y^2}$ symmetry, when gap on different pockets at points X change signs, while gaps on hole – like pockets are zero:

$$\Delta_1 = \Delta_2 = 0, \quad \Delta_3 = -\Delta_4 = \Delta, \tag{12}$$

$$g = (\mu - \lambda)\nu_3. \tag{13}$$

Possibility of such solution follows also from the general symmetry analysis [166].

2) two solutions, corresponding to the so called $s^{\pm}$ – pairing, when gaps at points X have the same sign, while gaps on Fermi surfaces, surrounding point Γ may have opposite sign, and

$$\begin{aligned} 2g_{+,-} \;=\; & -u(\nu_1+\nu_2) - (\lambda+\mu)\nu_3 \pm \\ & \sqrt{(u(\nu_1+\nu_2) - (\lambda+\mu)\nu_3)^2 + 8t^2\nu_3(\nu_1+\nu_2)} \end{aligned} \tag{14}$$

and[9]

$$\Delta_1 = \Delta_2 = \kappa\Delta, \quad \Delta_3 = \Delta_4 = \Delta, \tag{15}$$

where $\kappa^{-1} = -(g_{+,-} + u(\nu_1+\nu_2))/(t\nu_3)$.

For the first time possibility of $s^{\pm}$ – pairing in FeAs compounds was noted in Ref. [110]. This solution is in qualitative agreement with ARPES data [136, 137, 140], except the results $\Delta_1 = \Delta_2$ from (15), which contradicts the established fact – the gap on a small hole – like cylinder is approximately twice as large as on a big cylinder. In our opinion, this deficiency is due to unnecessary limitation of $u = V^{h1,h1} = V^{h2,h2} = V^{h1,h2}$, used in Ref. [166]. In case of different BCS constants on hole – like cylinders we can easily obtain different values of gaps in agreement with experiments.

The presence of practically isotropic gaps (possibly of different signs) on hole – like and electron – like pockets of the Fermi surface, corresponding to $s^{\pm}$ – pairing, seems at first to contradict NMR (NQR) data discussed above, which indicate possible gap d-wave gap symmetry. This contradiction was studied in Ref. [174], where it was shown rather convincingly that the absence of Gebel – Slicter peak and power like temperature dependence of NMR relaxation may be easily explained also in the case of $s^{\pm}$ – pairing, with an account of impurity scattering.

Electron – phonon mechanism

General discussion of the previous section tells us nothing about the origin of pairing coupling constants entering the matrix (8), i.e. about microscopic mechanism of Cooper pairing in new superconductors.

As a first candidate of such mechanism we have to consider the usual electron – phonon interaction. Such analysis for LaOFeAs was performed in Ref. [109], using ab initio calculations of electron and phonon spectra and Eliashberg function $\alpha^2 F(\omega)$, determining electron – phonon pairing constant as:

$$\lambda(\omega) = 2\int_0^{\omega} d\Omega \alpha^2 F(\Omega)/\Omega \tag{16}$$

[9] Here we have corrected small misprints of Ref. [166].

The total electron – phonon pairing constant λ was obtained by numerical integration in (16) up to $\omega = \infty$ and was found to be 0.21. To estimate superconducting critical temperature T_c we can use a popular Allen – Dynes interpolation formula [175]:

$$T_c = \frac{f_1 f_2 \omega_{ln}}{1.20} \exp\left(-\frac{1.04(1+\lambda)}{\lambda - \mu^* - 0.62\lambda\mu^*}\right), \tag{17}$$

where

$$f_1 = [1 + (\lambda/\Lambda_1)^{3/2}]^{1/3}, \qquad \Lambda_1 = 2.46(1 + 3.8\mu^*),$$
$$f_2 = 1 + \frac{(\bar{\omega}_2/\omega_{ln} - 1)\lambda^2}{\lambda^2 + \Lambda_2^2}, \qquad \Lambda_2 = 1.82(1 + 6.3\mu^*)(\bar{\omega}_2/\omega_{ln}), \qquad \bar{\omega}_2 = <\omega^2>^{1/2}$$

and $<\omega^2>$ is an average square of phonon frequency. Taking into account the value of average logarithmic frequency of phonons found in Ref. [109] $\omega_{ln} = 205K$ (and assuming $\omega_{ln} \approx \bar{\omega}_2$), with optimistic choice of Coulomb pseudopotential $\mu^* = 0$, (17) gives the value of $T_c = 0.5$K. Numerical solution of Eliashberg equations with calculated $\alpha^2 F(\omega)$ gave the value of $T_c = 0.8$K [109]. Actually, to reproduce the experimental value of $T_c = 26$K coupling constant λ should be approximately five times larger, even if we use $\mu^* = 0$. In opinion of the authors of Ref. [109] such a strong discrepancy clearly shows that the usual picture of Cooper pairing, based on electron – phonon coupling, is invalid.

Despite quite convincing estimates of Ref. [109] we should note, that these are based upon the standard approach of Eliashberg theory, which does not take into account, in particular, an important role of multi – band nature of superconductivity in these compounds, e.g. the importance of interband pairing interactions. Besides that, the estimates of the value of electron – phonon coupling constant has also met some objections. Thus, in Ref. [176] it was argued that strong enough coupling exists between electrons and a certain mode of Fe oscillations in FeAs plane.

However, probably most convincing objections to the claims of irrelevance of electron – phonon coupling can be based on experiments. For example, we can estimate the electron – phonon coupling constant from the temperature dependence of resistivity. In Ref. [177] the measurements of resistivity of $PrFeAsO_{1-x}F_x$ were done in a wide enough temperature interval. Linear growth of resistivity with temperature for $T >$170K saturated, which by itself suggests strong enough electron – phonon coupling. As a simple estimate we can write resistivity as:

$$\rho(T) = \frac{4\pi}{\omega_p^2 \tau} \tag{18}$$

where ω_p is plasma frequency, τ is carriers relaxation time. In the region of high enough temperatures, where resistivity grows linearly with temperature, relaxation frequency of carriers on phonons is given by [179]:

$$\frac{\hbar}{\tau_{ep}} = 2\pi\lambda_{tr} k_B T \tag{19}$$

where "transport" constant of electron – phonon coupling λ_{tr}, is naturally of the order of λ of interest to us, differing from it usually not more than by 10%. From (18) and (19) we have:

$$\lambda_{tr} = \frac{\hbar\omega_p^2}{8\pi^2 k_B} \frac{d\rho}{dT} \tag{20}$$

Using the slope of the temperature dependence of resistivity determined in Ref. [177] $d\rho/dT \sim 8.6$ ($\mu\Omega$/K) and the estimate of plasma frequency $\omega_p \sim 0.8$ eV (which follows from measurements of penetration depth), we get $\lambda \sim 1.3$, which according to (17) is quite sufficient to get the observable values of transition temperatures in new superconductors.

Decisive evidence for electron – phonon mechanism of Cooper pairing was always considered to be the observation of isotope effect. Appropriate measurements were performed recently in Ref. [178] on $SmFeAsO_{1-x}F_x$, where ^{16}O was substituted by ^{18}O, and on $Ba_{1-x}K_xFe_2As_2$, where ^{56}Fe was substituted by ^{54}Fe. A finite shift of superconducting transition temperature was observed, which can be characterized in a standard way by isotope effect exponent $\alpha = -\frac{d\ln T_c}{d\ln M}$. For $SmFeAsO_{1-x}F_x$ isotope effect was small enough, with $\alpha \sim 0.08$, which is quite natural as O ions are outside the conducting FeAs layer. At the same time, the change of Fe ions in FeAs layers in $Ba_{1-x}K_xFe_2As_2$ has lead to a large isotope effect with $\alpha \approx 0.4$, which is close to the "ideal" value of $\alpha = 0.5$.

Thus, rather wide pessimism in the literature on the role of electron – phonon interaction in new superconductors seems to be rather premature.

Magnetic fluctuations

The pessimism with respect to the role of electron – phonon interaction mentioned above, as well as the closeness of superconducting phase to antiferromagnetic on the phase diagram of new superconductors, has lead to the growth of popularity of pairing models based upon the decisive role of magnetic (spin) fluctuations, in many respects similar to those already considered for HTSC cuprates [4, 5].

Apparently, one of the first papers where the possible role of magnetic fluctuations in formation of Cooper pairs of $s^{\pm}$ – type was stressed on qualitative level was Ref. [110]. Similar conclusions were reached by the authors of Ref. [124], where a possibility of $d_{x^2-y^2}$ – pairing was also noticed.

Rather detailed analysis of possible electronic mechanisms of pairing within the generalized Hubbard model applied to the "minimal" model of Ref. [127] was performed in Ref. [180]. In fact, this analysis was done in the framework of generalized RPA approximation, which takes into account an exchange by spin (and orbital) fluctuations in particle – hole channel (cf. the review of similar one – band models used for cuprates [4]). It was shown that the pairing interaction due to these fluctuations leads to effective attraction in case of singlet d-wave pairing and triplet p-wave pairing, with tendency to d-wave pairing instability becoming stronger as system moves towards magnetic (SDW) instability. In rather general formulation, using the general renormalization group approach, the similar model was analyzed in Ref. [181].

Unfortunately, in most of the papers devoted to pairing mechanism due to exchange of magnetic fluctuations there are no direct calculations of T_c allowing comparison with experiments. Thus we shall limit ourselves to these short comments.

CONCLUSION: END OF CUPRATE MONOPOLY

Let us briefly summarize. During the first half a year of studies of new superconductors we have observed rather impressive progress in learning on their basic physical properties. Very few problems remain uninvestigated, though many results obtained require further clarification[10]. The main result of all these studies is certainly the end of cuprate monopoly in physics of high – temperature superconductors. A new wide class of iron based systems was discovered with high enough values of T_c and variety of physical properties which reminds copper oxides, which for more than 20 years were in the center of interests of superconductor community. There are rather well founded expectations that in some near future new systems will be discovered, though there is now a certain impression that in the subclass of layered FeAs systems we have already reached the maximum values of $T_c \sim 50$K, so that for further enhancement of T_c we need some kind of a new approaches. It is doubtless that work already done significantly deepened our understanding of the nature of high – temperature superconductivity, though we are still far from formulation of definite "recipies" for the search of new superconductors with higher values of T_c.

Let us formulate

What is in common between iron based and cuprate superconductors?

- Both classes are represented by quasi two – dimensional (layered) systems from the point of view of their electronic properties, which leads to more or less strong anisotropy.
- In both classes superconducting region on the phase diagram is close to the region of antiferromagnetic ordering. Prototype phase for both classes of superconductors is antiferromagnetic.
- Cooper pairing in both classes is singlet type, but "anomalous", i.e. different from simple s-wave pairing, characteristic for traditional (low – temperature) superconductors.
- Basic properties of superconducting state is more or less the same as in typical type II superconductors.

---

[10] In this respect we want to stress the absence of any systematic studies of effects of disordering, which may be unusual due to anomalous nature of $s^{\pm}$ – pairing

From the point of view of our understanding of basic nature of high – temperature superconductivity the meaning of these common properties remains rather unclear. Why do we need (and do we need?) two – dimensionality? Historically, the importance of two – dimensionality was first stressed in connection with the proposed high – temperature superconductivity based on excitonic mechanism of Ginzburg and Little [182], but does it play any significant role for superconductivity in cuprates and new iron based superconductors? Do we need "closeness" to antiferromagnetism? Is antiferromagnetism just a competing phase, or it is helpful for HTSC, e.g. via the replacement of electron – phonon pairing by mechanism based upon spin (antiferromagnetic) fluctuations? The answers to these questions are still unclear, though the presence of such coincidences in rather different classes of physical systems seem rather significant.

Let us look now

What is different between iron based and cuprate superconductors?

- Prototype phases of HTSC cuprates are antiferromagnetic (strongly correlated, Mott type) insulators, while for new superconductors these are antiferromagnetic (intermediately correlated?) metals.
- Cuprates in superconducting state are one band metals with a single Fermi surface (hole – like or electron – like), while new superconductors are multiple band metals with several hole – like and electron – like Fermi surfaces.
- In cuprates we have anisotropic d-wave pairing, while in new superconductors, almost surely, we have (almost?) isotropic $s^{\pm}$ – pairing.
- It is quite possible that the microscopic mechanism of pairing in both classes of superconductors is different — in cuprates it is almost certainly electronic mechanism (spin fluctuations), while in iron based superconductors the role of electron – phonon coupling can be quite important (isotope effect!).

We see that differences between cuprates and new superconductors are probably more pronounced than common properties. In this sense, one of the main conclusions which can already be made is that HTSC is not a unique property of cuprates, i.e. strongly correlated systems close to insulating state. In some respects new superconductors are simpler and easier to understand — their normal state is not so mysterious as in the case of cuprates[11], though multiple band structure complicates situation.

To conclude, we can expect that high – temperature superconductivity is much more common, than it was assumed during the last 20 years, so that superconducting community may look into the future with certain optimism.

The author is grateful to L.P. Gor'kov and I.I. Mazin for numerous discussions on physics of new superconductors. He is also grateful to I.A. Nekrasov and Z.V. Pchelkina who co-authored papers on calculations of electronic spectra of FeAs based systems. This work was partly supported by Russian Foundation of Basic Research grant 08-02-00021 and by the programs of fundamental research of the Russian Academy of Sciences "Quantum macrophysics" and "Strongly correlated electrons in semiconductors, metals, superconductors and magnetic materials".

[1] J.G. Bednorz, K.A. Müller. Zs. Phys. **64**, 189 (1986)
[2] L.P. Gor'kov, N.B. Kopnin. Usp. Fiz. Nauk (Physics - Uspekhi) **156**, 117 (1988)
[3] Yu.A. Izyumov, N.M. Plakida, Yu.N. Skryabin. Usp. Fiz. Nauk (Physics Uspekhi) **159**, 621 (1989)
[4] Yu.A. Izyumov. Usp. Fiz. Nauk (Physics Uspekhi) **161**, 63 (1991)
[5] Yu.A. Izyumov. Usp. Fiz. Nauk (Physics Uspekhi) **169**, 225 (1999)
[6] E.G. Maksimov. Usp. Fiz. Nauk (Physics Uspekhi) **170**, 1033 (2000)
[7] M.V. Sadovskii. Usp. Fiz. Nauk **171**, 539 (2001); Physics Uspekhi **44**, 515 (2001)
[8] V.N. Belyavskii, Yu.V. Kopaev. Usp. Fiz. Nauk (Physics Uspekhi) **176**, 457 (2006)
[9] E.G. Maksimov. Usp. Fiz. Nauk (Physics Uspekhi) **178**, 175 (2008)

[11] Some evidence for the pseudogap state is observed only in NMR data and it is unclear, whether in new superconductors we have an additional pseudogap region on the phase diagram as in cuprates, with appropriate renormalization of electronic spectrum, like formation of "Fermi arcs" etc.

[10] Yu.V. Kopaev. Usp. Fiz. Nauk (Physics Uspekhi) **178**, 202 (2008)
[11] N.M. Plakida. High – Temperature Superconductors. Moscow 1996
[12] P.W. Anderson. The Theory of Superconductivity in the High-T_c Cuprates. Princeton University Press, 1997
[13] Handbook of High-Temperature Superconductivity. Ed. by J.R. Schrieffer. Springer, 2007
[14] Superconductivity. In 2 volumes. Ed. by K.H. Bennemann and J.B. Ketterson. Springer, 2008
[15] Y. Kamihara, T. Watanabe, M. Hirano, H. Hosono. J. Am. Chem. Soc. **130**, 3296 (2008)
[16] H. Shaked, P.M. Keane, J.C. Rodriguez, F.F. Owen, R.L. Hitterman, J.D. Jorgensen. Crystal Structures of the High-Tc Superconducting Copper-Oxides. Elsevier Science B.V. 1994
[17] M.V. Sadovskii. Models of the pseudogap state in high – temperature superconductors. In "Strings, branes, lattices, nets, pseudogaps and dust" (Proc. I.E. Tamm seminar), p.p. 357-441. Scientific World, Moscow 2007, arXiv: cond-mat/0408489
[18] S. Hüfner, M.A. Hossain, A. Damascelli, G.A. Sawatzky. Rep. Prog. Phys. **71**, 062501 (2008)
[19] C.H. Pennington, V.A. Stenger. Rev. Mod. Phys. **68**, 855 (1996)
[20] A.P. Mackenzie, Y. Maeno. Rev. Mod. Phys. **75**, 657 (2003)
[21] S.G. Ovchinnikov. Usp. Fiz. Nauk (Physics Uspekhi) **173**, 27 (2003)
[22] K. Vinod, N. Varghese, U. Suyamaprasad. Supercond. Sci. Technol. **20**, R31 (2007)
[23] M. Putti, R. Vaglio, J.M. Rowell. Supercond. Sci. Technol. **21**, 043001 (2008)
[24] Y. Kamihara, H. Hiramatsu, M. Hirano, R. Kawamura, H. Yanagi, T. Kamiya, H. Hosono. J. Am. Chem. Soc. **128**, 10012 (2006)
[25] T. Watanabe, H. Yanagi, T. Kamiya, Y. Kamihara, H. Hiramatsu, M. Hirano, H. Hosono. Inorg. Chem. **46**, 7719 (2006)
[26] G.F. Chen, Z. Li, G. Li, J. Zhou, D. Wu, J. Dong, W.Z. Hu, P. Zheng, Z.J. Chen, J.L. Luo, N.L. Wang. Phys. Rev. Lett. **101**, 057007 (2008); arXiv: 0803.0128
[27] Xiyu Zhu, Huan Yang, Lei Fang, Gang Mu, Hai-Hu Wen. Supercond. Sci. Technol. **21**, 105001 (2008); arXiv: 0803.0128
[28] A.S. Sefat, M.A. McGuire, B.C. Sales, Rongying Jin, J.Y. Howe, D. Mandrus. Phys. Rev. B **77**, 174503 (2008); arXiv: 0803.2528
[29] X.H. Chen, T. Wu, G. Wu, R.H. Liu, H. Chen, D.F. Fang. Nature **453**, 761 (2008); arXiv: 0803.3603
[30] G.F. Chen, Z. Li, D. Wu, G. Li, W.Z. Hu, J. Dong, P. Zheng, J.L. Luo, N.L. Wang. Phys. Rev. Lett. **100**, 247002 (2008); arXiv: 0803.3790
[31] Zhi-An Ren, Jie Yang, Wei Lu, Wei Yi, Xiao-Li Shen, Zheng-Cai Li, Guang-Can Che, Xiao-Li Dong, Li-Ling Sun, Fang Zhou, Zhong-Xian Zhao. Europhys. Lett. **82**, 57002 (2008); arXiv: 0803.4234
[32] G.F. Chen, Z. Li, D. Wu, J. Dong, G. Li, W.Z. Hu, P. Zheng, J.L. Luo, N.L. Wang. Chin. Phys. Lett. **25**, 2235 (2008); arXiv: 0804.4384
[33] Zhi-An Ren, Guang-Can Che, Xiao-Li Dong, Jie Yang, Wei Lu, Wei Yi, Xiao-Li Shen, Zheng-Cai Li, Li-Ling Sun, Fang Zhou, Zhong-Xian Zhao. Europhys. Lett. **83**, 17002 (2008); arXiv: 0804.2582
[34] Wei, Xiao-Li Shen, Jie Yang, Zheng-Cai Li, Wei Yi, Zhi-An Ren, Xiao-Li Dong, Guang-Can Che, Li-Ling Sun, Fang Zhou, Zhong-Xian Zhao. Sol. State Comm. **148**, 168 (2008); arXiv: 0804.3725
[35] Jie Yang, Zheng-Cai Li, Wei Lu, Wei Yi, Xiao-Li Shen, Zhi-An Ren, Guang-Can Che, Xiao-Li Dong, Li-Ling Sun, Fang Zhou, Zhong-Xian Zhao. Supercond. Sci. Technol. **21**, 082001 (2008); arXiv: 0804.3727
[36] Hai-Hu Wen, Gang Mu, Lei Fang, Huan Yang, Xiyu Zhu. Europhys. Lett. **82**, 17009 (2008); arXiv: 0803.3021
[37] Cao Wang, Linjun Li, Shun Chi, Zengwei Zhu, Zhi Ren, Yuke Li, Yuetao Wang, Xiao Lin, Yongkang Luo, Xiangfan Xu, Guanghan Cao, Zhu'an Xu, arXiv: 0804.4290
[38] H. Takahashi, K. Igawa, K. Arii, Y. Kamihara, M. Hirano, H. Hosono. Nature doi:10.1038/nature06972
[39] D.A. Zocco, J.J. Hamlin, R.E. Baumbach, M.B. Maple, M.A. McGuire, A.S. Sefat, B.C. Sales, R. Jin, D. Mandrus, J.R. Jeffries, S.T. Weir, Y.K. Vohra. Physica C ( ); arXiv: 0805.4372
[40] G. Garbarino, P. Toulemonde, M. Alvarez-Murga. A. Sow, M. Mezouar, M. Nunez-Regueiro, arXiv: 0808.1132
[41] M. Tegel, S. Johansson, V. Weiss, I. Schellenberg, W. Hermes, R. Poettgen, D. Johrendt, arXiv:0810.2120v1.
[42] F. Han, X. Zhu, G. Mu, P. Cheng, H.H. Wen, arXiv:0810.2475v1.
[43] S. Matsuishi, Y. Inoue, T. Nomura, M. Hirano, H. Hosono, arXiv:0810.2351v1.
[44] X. Zhu, F. Han, P. Cheng, G. Mu, B. Shen, Hai-Hu Wen, arXiv:0810.2531v2.
[45] M. Rotter, M. Tegel, D. Johrendt. Phys. Rev. Lett **101**, 107006 (2008); arXiv: 0805.4630.
[46] M. Rotter, M. Tegel, D. Johrendt. Phys. Rev. B**78**, 020503 (2008); arXiv: 0805.4021.
[47] T. Nomura, S. W. Kim, Y. Kamihara, M. Hirano, P. V. Sushko, K. Kato, M. Takata, A. L. Shluger, H. Hosono, arXiv: 0804.3569.
[48] G.F. Chen, Z. Li, G. Li, W.Z. Hu, J. Dong, X.D. Zhang, P. Zheng, N.L. Wang, J.L. Luo. Chin. Phys. Lett. **25**, 3403 (2008); arXiv: 0806.1209
[49] P. Alireza, J. Gillett, Y.T. Chris Ko, S.E. Sebastian, G. Lonzarich. J. Phys. Cond. Matter ( ); arXiv: 0807.1896
[50] A.S. Sefat, R. Jin, M.A. McGuire, B.C, Sales, D.J. Singh, D. Mandrus. Phys. Rev. Lett. **101**, 117004 (2008); arXiv: 0807.3370
[51] K. Sasmal, B. Lv, B. Lorenz, A. Guloy, F. Chen, Y. Xue, C.W. Chu. Phys. Rev. Lett. **101**, 107007 (2008); arXiv: 0806.1301
[52] X.C. Wang, Q.Q. Liu, Y.X. Lv, W.B. Gao, L.X. Yang, R.C. Yu, F.Y. Li, C.Q. Jin, arXiv: 0806.4688
[53] J.H. Tapp, Z. Tang, B. Lv, K. Sasmal, B. Lorenz, C.W. Chu, A.M. Guloy, Phys. Rev. B **78**, 060505 (2008); arXiv: 0807.2274
[54] Fong-Chi Hsu, Jiu-Yong Luo, Kuo-Wei Yeh, Ta-Kun Chen, Tzu-Wen Huang, P.M. Wu, Yong-Chi Lee, Yi-Lin Huang, Yan-Yi Chu, Der-Chung Yan, Maw-Kuen Wu, arXiv: 0807.2369

[55] Y. Mizuguchi, F. Tomioka, S. Tsuda, T. Yamaguchi, Y. Takano, arXiv: 0807.4315
[56] M.H. Fang, H.M. Pham, B. Qian, T.J. Liu, E.K. Vehstedt, Y. Liu, L. Spinu, Z.Q. Mao, arXiv: 0807.4775
[57] V.L. Kozhevnikov, O.N. Leonidova, A.L. Ivanovskii, I.R. Shein, B.N. Goshchitskii, A.E. Kar'kin. Pis'ma v ZhETF (JETP Letters) **87**, 747 (2008); arXiv: 0804.4546
[58] Junyi Ge, Shixum Cao, Jincang Zhang, arXiv: 0807.5045
[59] Z. Li, G.F. Chen. J. Dong, G. Li, W.Z. Hu, D. Wu, S.K. Su, P. Zheng, T. Xiang, N.L. Wang, J.L. Luo. Phys. Rev. B **78**, 060504 (2008); arXiv: 0803.2572
[60] F. Ronning, N. Kurita, E.D. Bauer, B.L. Scott, T. Park, T. Klimczuk, R. Movshovich, J.D. Thomson. J. Phys. Condens. Matter **20**, 342203 (2008); arXiv: 0807.3788
[61] T. Klimczuk, T.M. McQueen, A.J. Williams, Q. Huang, F. Ronning, E.D. Bauer, J.D. Thompson, M.A. Green, R.J. Cava, arXiv: 0808.1557
[62] T.C. Ozawa, S.M. Kauzlarich. Sci. and Technol. Adv. Materials. **9**, No. 3 (2008); arXiv: 0808.1158
[63] N.D. Zhigadlo, S. Katrych, Z. Bukowski, S. Weyeneth, R. Puzniak, J. Karpinski. J. Phys. Condens. Matter **20**, 342202 (2008); arXiv: 0806.0337
[64] Ying Jia, Peng Cheng, Lei Fang, Huiqian Luo, Huan Yang, Cong Ren, Lei Shan, Chanzhi Gu, Hai-Hu Wen. Appl. Phys. Lett. **93**, 032503 (2008); arXiv: 0806.0532
[65] N. Ni, S.L. Bud'ko, A. Kreyssig, S. Nandi, G.E. Rustan, A.I. Goldman, S. Gupta, J.D. Corbett, A. Kracher, P.C. Canfield. Phys. Rev. B **78**, 014507 (2008); arXiv: 0806.1874
[66] S.B. Zhang, Y.P. Sun, X.D. Zhu, X.B. Zhu, B.S. Wang, G. Li, H.C. Lei, X. Luo, Z.R. Yang, W.H. Soong, J.M. Dai, arXiv: 0809.1905
[67] X.F. Wang, T. Wu, G. Wu, H. Chen, Y.L. Xie, J.J. Ying, Y.J. Yan, R.H. Liu, X.H. Chen, arXiv: 0806.2452
[68] H.Q. Yuan, J. Singleton, F.F. Balakirev, G.F. Chen, J.L. Luo, N.L. Wang, arXiv: 0807.3137
[69] C. de la Cruz, Q. Huang, J.W. Lynn, Jiying Li, W. Ratcliff II, J.L. Zaretsky, H.A. Mook, G.F. Chen, J.L. Luo, N.L. Wang, Pengcheng Dai. Nature **453**, 899 (2008); arXiv: 0804.0795
[70] H. Luetkens, H.-H. Klauss, M. Kraken, F.J. Litterst, T. Dellmann, R. Klingeler, C. Hess, R. Khasanov, A. Amato, C. Baines, J. Hamann-Borrero, N. Leps, A. Kondrat, G. Behr, J. Werner, B. Büchner, arXiv: 0806.3533
[71] Jun Zhao, Q. Huang, C. de la Cruz, Shiliang Li, J.W. Lynn, Y. Chen, M.A. Green, G.F. Chen, G. Li, J.L. Luo, N.L. Wang, Pengcheng Li, arXiv: 0806.2528
[72] J.T. Markert, Y. Dalichaouch, M.B. Maple. In "Physical Properties of High Temperature Superconductors I". Ed. by D.M. Ginsberg, World Scientific, Singapore, 1989
[73] Y. Qiu, Wei Bao, Q. Huang, J.W. Lynn, T. Yildrim, J. Simmons, Y.C. Gasparovic, J. Li, M. Green, T. Wu, G. Wu, X.H. Chen, arXiv: 0806.2195
[74] Ying Chen, J.W. Lynn, J. Li, G. Li, G.F. Chen, J.L. Luo, N.L. Wang, Pengcheng Dai, C. de la Cruz, H.A. Mook. Phys. Rev. B **78**, 064515 (2008); arXiv: 0807.0662
[75] A.J. Drew, Ch. Niedermayer, P.J. Baker, F.L. Pratt, S.J. Blundell, T. Lancaster, R.H. Liu, G. Wu, X.H. Chen, I. Watanabe, V.K. Malik, A. Dubroka, M. Rössle, K.W. Kim, C. Baines, C. Bernard, arXiv: 0807.4876
[76] Q. Huang, Y. Qiu, Wei Bao, J.W. Lynn, M.A. Green, Y.C. Gasparovic, T. Wu, G. Wu, X.H. Chen, arXiv: 0806.2776
[77] Jun Zhao, W. Ratcliff II, J.W. Lynn, G.F. Chen, J.L. Luo, N.L. Wang, Jiangping Hu, Pengcheng Dai, arXiv: 0807.1077
[78] H. Chen, Y. Ren, Y. Qiu, Wei Bao, R.H. Liu, G. Wu, T. Wu, Y.L. Xie, X.F. Wang, Q. Huang, X.H. Xhen, arXiv: 0807.3950
[79] Wei Bao, Y. Qiu, Q. Huang, M.A. Green, P. Zajdel, M.R. Fitzsimmons, M. Zhernenkov, Minghu Fang, B. Qian, E.K. Vehstedt, Jinhu Yang, H.M. Pham, L. Spinu, Z.Q. Mao, arXiv: 0809.2058
[80] L. Ding, C. He, J.K. Dong, T. Wu, R.H. Liu, X.H. Chen, S.Y. Li. Phys. Rev. B **77**, 180510 (2008); arXiv: 0804.3642
[81] J.K. Dong, L. Ding, H. Wang, X.F. Wang, T. Wu, X.H. Chen, S.Y. Li, arXiv: 0806.3573
[82] Gang Mu, Huiqian Luo, Zhaosheng Wang, Lei Shan, Cong Ren, Hai-Hu Wen, arXiv: 0808.2941
[83] Y. Nakai, K. Ishida, Y. Kamihara, M. Hirano, H. Hosono. J. Phys. Soc. Japan **77**, 073701 (2008); arXiv: 0804.4765
[84] H. Mukuda, N. Terasaki, H. Kinouchi, M. Yashima, Y. Kitaoka, S. Suzuki, S. Miyasaka, S. Tajima, K. Miyazawa, P. Shirage, H. Kito, H. Eisaki, A. Iyo. J. Phys. Soc. Japan **77**, 093704 (2008); arXiv: 0806.3238
[85] K. Matano, Z.A. Ren, X.L. Ding, X.L. Dong, L.L. Sun, Z.X. Zhao, Guo-qing Zheng. Europhys. Lett **83**, 570001 (2008); arXiv: 0806.0249
[86] H. Fukuzawa, K. Hirayama, K. Kondo, T. Yamazaki, Y. Kohori, N. Takeshita, K. Miyazawa, H. Kito, H. Eisaki, A. Iyo. J. Phys. Soc. Japan **77**, 093706 (2008); arXiv: 0806.4514
[87] F.L. Ning, K. Ahilan, T. Imai, A.S. Sefat, R. Jin, M.A. McGuire, B.C. Sales, D. Mandrus. J. Phys. Soc. Japan **77**, 103705; arXiv: 0808.1420
[88] H. Kotegawa, S. Masaki, Y. Awai, H. Tou, Y. Mizugichi, Y. Takano, arXiv: 0808.0040
[89] T.Y. Chen, Z. Tesanovic, R.H. Liu, X.H. Chen, C.L. Chien. Nature **453**, 1224 (2008); arXiv: 0805.4616
[90] O. Millo, I. Asulin, O. Yuli, I. Felner, Z.-A. Ren, X.-L. Shen, G.-C. Che, Z.-X. Zhao, arXiv: 0807.0359
[91] M.H. Pan, X.B. He, G.R. Li, J.F. Wendelken, R. Jin, A.S. Sefat, M.A. NcGuire, B.C. Sales, D. Mandrus, E.W. Plummer, arXiv: 0808.0895
[92] Yong-Lei Wang, Lei Shan, Lei Fang, Peng Cheng, Cong Ren, Hai-Hu Wen, arXiv: 0806.1986
[93] A. Dubroka, K.W. Kim, M. Rössle, V.K. Malik, R.H. Liu, G. Wu, X.H. Chen, C. Bernard. Phys. Rev. Lett. **101** 097011 (2008); arXiv: 0805.2415
[94] A.V. Boris, N.N. Kovaleva, S.S.A. Seo, J.S. Kim, P. Popovich, Y. Matiks, R.K. Kremer, B. Keimer, arXiv: 0806.1732
[95] J. Yang, D. Hüvonen, U. Nagel, T. Rõõm, N. Ni, P.C. Canfield, S.L. Bud'ko, J.P. Carbotte, T. Timusk, arXiv: 0807.1040

[96] G. Li, W.Z. Hu, J. Dong, Z. Li, P. Sheng, G.F. Chen, J.L. Luo, N.L. Wang. Phys. Rev. Lett. **101**, 107004 (2008); arXiv: 0807.1094

[97] R. A. Ferrell and R. E. Glover, III, Phys. Rev. **109**, 1398 (1958)

[98] M. Tinkham and R. A. Ferrell, Phys. Rev. Lett. **2**, 331 (1959)

[99] Y. Qiu, M. Kofu, Wei Bao, S.-H. Lee, Q. Huang, T. Yildrim, J.R.D. Copley, J.W. Lynn, T. Wu, G. Wu, X.H. Chen. Phys. Rev. B **78**, 052508 (2008); arXiv: 0805.1062

[100] A.D. Christianson, M.D. Lumsden, O. Delaire, M.B. Stone, D.L. Abernathy, M.A. McGuire, A.S. Sefat, R. Jin, B.C. Sales, D. Mandrus, E.D. Mun, P.C. Canfield, J.Y.Y. Lin, M. Lucas, M. Kresh, J.B. Keith, B. Fultz, E.A. Goremychkin, R.J. McQueeney, arXiv: 0807.3370

[101] D.J. Singh, M.H. Du. Phys. Rev. Lett. **100**, 237003 (2008); arXiv: 0803.0429

[102] S. Higashitaniguchi, M. Seto, S. Kitao, Y. Kobayashi, M. Saito, R. Masuda, T. Mitsui, Y. Yoda, Y. Kamihara, M. Hirano, H. Hosono, arXiv: 0807.3968

[103] T. Fukuda, A.Q.R. Baron, S. Shamoto, M. Ishikado, H. Nakamura, M. Machida, H. Uchiyama, S. Tsutsui, A. Iyo, H. Kito, J. Mizuki, M. Arai, H. Eisaki, Y. Matsuda, H. Hosono, arXiv: 0808.0838

[104] R. Mittal, Y. Su, S. Sols, T. Chatterji, S.L. Chaplot, H. Schober, M. Rotter, D. Johrendt, Th. Brueckel. Phys. Rev. B **78**, 104514 (2008); arXiv: 0807.3172

[105] M. Sbiri, H. Schober, M.R. Johnson, S. Rols, R. Mittal, Y. Su, M. Rotter, D. Johrendt, arXiv: 0807.4429

[106] J. Zhao, D.-X. Yao, S. Li, T. Hong, Y. Chen, S. Chang, W. Ratcliff II, J.W. Lynn, H.A. Mook, G.F. Chen, J.L. Luo, N.L. Wang, E.W. Carlson, J. Hu, P. Dai, arXiv: 0808.2455

[107] R.A. Ewings, T.G. Perring, R.I. Bewley, T. Guidi, M.J. Pitcher, D.R. Parker, S.J. Clarke, A.T. Boothroyd, arXiv: 0808.2836

[108] S. Lebègue, Phys. Rev. B 75, 035110 (2007).

[109] L. Boeri, O.V. Dolgov, A.A. Golubov. Phys. Rev. Lett. **101**, 026403 (2008); arXiv: 0803.2703v1

[110] I.I. Mazin, D.J. Singh, M.D. Johannes, M.H. Du. Phys. Rev. Lett. **101**, 057003 (2008); arXiv: 0803.2740

[111] G. Xu, W. Ming, Y. Yao, Xi Dai, S.-C. Zhang, Z. Fang. Europhys. Lett. **82**, 67002 (2008); arXiv: 0803

[112] I.R. Shein, A.L. Ivanovskii. **88**, 115 (2008); arXiv: 0806.0750

[113] F. Ma, Z.-Y. Lu, T. Xiang, arXiv: 0806.3526

[114] D.J. Singh. Phys. Rev. B **78**, 094511 (2008); arXiv: 0807.2643

[115] I.R. Shein, A.L. Ivanovskii. Pis'ma v ZhETF (JETP Letters) **88**, 377 (2008)

[116] A. Subedi, L. Zhang, D.J. Singh, M.H. Du, arXiv: 0807.4312

[117] I.A. Nekrasov, Z.V. Pchelkina, M.V. Sadovskii. Pis'ma v ZhETF **87**, 647 (2008); JETP Letters **87**, 620 (2008); arXiv: 0804.1239

[118] I.A. Nekrasov, Z.V. Pchelkina, M.V. Sadovskii. Pis'ma v ZhETF **88**, 155 (2008); JETP Letters **88**, 144 (2008); arXiv: 0806.2630

[119] I.A. Nekrasov, Z.V. Pchelkina, M.V. Sadovskii. Pis'ma v ZhETF **88**, 621 (2008); JETP Letters **88**, 543 (2008); arXiv: 0807.1010

[120] I.A. Nekrasov, Z.V. Pchelkina, M.V. Sadovskii. Pis'ma v ZhETF (JETP Letters) **88**, 777 (2008); arXiv: 0810.3377

[121] I.R. Shein, A.L. Ivanovskii, arXiv: 0810.3498

[122] O.K. Andersen. Phys. Rev. B **12**, 3060 (1975); O. Gunnarsson, O. Jepsen, O.K. Andersen. Phys. Rev. B **27**, 7144 (1983); O.K. Andersen, O. Jepsen. Phys. Rev. Lett. **53**, 2571 (1984)

[123] B.N. Goshchitskii, V.L. Kozhevnikov, M.V. Sadovskii. Int. J. Mod. Phys. B **2**, 1331 (1988)

[124] K. Kuroki, S. Onari, R. Arita, H. Usui, Y. Tanaka, H. Kontani, H. Aoki. Phys. Rev. Lett. **101**, 087004 (2008); arXiv: 0803.3325

[125] S.V. Chong, T. Mochiji, K. Kadowaki, arXiv: 0808.0288

[126] J. Yang, X.-L. Shen, W. Lu, W. Yi, Z.-C. Li, Z.-A. Ren, G.-C. Che, X.-L. Dong, L.-l. Sun, F. Zhou, Z.-X. Zhao, arXiv: 0809.3582

[127] S. Raghu, Xiao-Liang Qi, Chao-Xing Liu, D.J. Scalapino, Shou-Cheng Zhang. Phys. Rev. B **77**, 220503 (2008); arXiv: 0804.1113

[128] C. Cao, P.J. Hirschfeld, H.-P. Cheng. Phys. Rev. B **77**, 220506 (2008); arXiv: 0803.3236v1

[129] K. Kuroki, S. Onari. R. Arita, H. Usui, Y. Tanaka, H. Kontani, H. Aoki. Phys. Rev. Lett. **101**, 087004 (2008); arXiv: 0803.3325

[130] M.M. Korshunov, I. Eremin, arXiv: 0804.1793

[131] C. Liu, T. Kondo, M. Tillman, M. Tillman, G.D. Samolyuk, Y. Lee, C. Martin, J.L. McChesney, S. Bud'ko, M. Tanatar, E. Rotenberg, P. Canfield, R. Prozorov, B. Harmon, A. Kaminski, arXiv: 0806.2147

[132] L.X. Yang, H.W. Ou, J.F. Zhao, Y. Zhang, D.W. Shen, B. Zhou, J. Wei, F. Chen, M. Xu, C. He, X.F. Wang, T. Wu, G. Wu, Y. Chen, X.H. Chen, Z.D. Wang, D.L. Feng, arXiv: 0806.2627

[133] C. Liu, G.D. Samolyuk, Y. Lee, N. Ni, T. Kondo, A.F. Santander-Syro, S.L. Bud'ko, J.L. McChesney, E. Rotenberg, T. Valla, A.V. Fedorov, P.C. Canfield, B.N. Harmon, A. Kaminski, arXiv: 0806.3453

[134] H. Liu, W. Zhang, L. Zhao, X. Jia, J. Meng, G. Liu, X. Dong, G.F. Chen, J.L. Luo, N.L. Wang, W. Lu, G. Wang, Y. Zhou, Y. Zhu, X. Wang, Z. Xu, C. Chen, X.J. Zhou, arXiv: 0806.4802

[135] L. Zhao, H. Liu, W. Zhang, J. Meng, X. Jia, G. Liu, X. Dong, G.F. Chen, J.L. Luo, N.L. Wang, W. Lu, G. Wang, Y. Zhou, Y. Zhu, X. Wang, Z. Zhao, Z. Xu, C. Chen, X.J. Zhou, arXiv: 0807.0398

[136] H. Ding, P. Richard, K. Nakayama, T. Sugawara, T. Arakane, Y. Sekiba, A. Takayama, S. Souma, T. Sato, T. Takahashi, Z. Wang, X. Dai, Z. Fang, G.F. Chen, J.L. Luo, N.L. Wang. Europhys. Lett. **83**, 47001 (2008); arXiv: 0807.0419

[137] L. Eray, D. Qian, D. Hsiech, Y. Xia, L. Li, J.G. Checkelsky, A. Pasupathy, K.K. Gomes, A.V. Fedorov, G.F. Chen, J.L. Luo, A. Yazdani, N.P. Ong, N.L. Wang, M.Z. Hasan, arXiv: 0808.2185

[138] Y. Zhang, J. Wei, H.W. Ou, J.F. Zhao, B. Zhou, F. Chen, M. Xu, C. He, G. Wu, H. Chen, M. Arita, K. Shimada, H. Namatame, M. Taniguchi, X.H. Chen, D.L. Feng, arXiv: 0808.2738

[139] V.B. Zabolotnyy, D.S. Inosov, D.V. Evtushinsky, A. Koitzsch, A.A. Kordyuk, J.T. Park, D. Haug, V. Hinkov, A.V. Boris, D.L. Sun, G.L. Sun, C.T. Lin, B. Keimer, M. Knupfer, B. Büchner, A. Varykhalov, R. Follath, S.V. Borisenko, arXiv: 0808.2454

[140] D.V. Evtushinsky, D.S. Inosov, V.B. Zabolotnyy, A. Koitzsch, M. Knupfer, B. Büchner, G.L. Sun, V. Hinkov, A.V. Boris, C.T. Lin, B. Keimer, A. Varykhalov, A.A. Kordyuk, S.V. Borisenko, arXiv: 0809.4455

[141] T. Sato, K. Nakayama, Y. Sekiba, P. Richard, Y.-M. Xu, S. Souma, T. Takahashi, G.F. Chen, J.L. Luo, N.L. Wang, H. Ding, arXiv: 0810.3047

[142] A. Damascelli, Z. Hussain, Z.-X. Shen. Rev. Mod. Phys. **75**, 473 (2003)

[143] S.E. Sebastian, J. Gillett, N. Harrison, C.H. Mielke, S.K. Goh, P.H.C. Lau, G.G. Lonzarich, arXiv: 0806.4726

[144] A.I. Coldea, J.D. Fletcher, A. Carrington, J.G. Analytis, A.F. Bangura, J.-H. Chu, A.S. Erickson, I.R. Fisher, N.E. Hussey, R.D. McDonald, arXiv: 0807.4890

[145] W. Metzner and D. Vollhardt, Phys. Rev. Lett. **62**, 324 (1989).

[146] D. Vollhardt, in *Correlated Electron Systems*, edited by V. J. Emery, World Scientific, Singapore, 1993, p. 57.

[147] Th. Pruschke, M. Jarrell, and J. K. Freericks, Adv. in Phys. **44**, 187 (1995).

[148] Yu.A. Izyumov. Usp. Fiz. Nauk (Physics Uspekhi) **165**, 403 (1995)

[149] A. Georges, G. Kotliar, W. Krauth, and M. J. Rozenberg, Rev. Mod. Phys. **68**, 13 (1996).

[150] G. Kotliar and D. Vollhardt, Physics Today **57**, No. 3 (March), 53 (2004).

[151] G. Kotliar, S.Y. Savrasov, K.Haule, V.S. Oudovenko, O. Parcollet, C.A. Marinetti. Rev. Mod. Phys. **78**, 865 (2006)

[152] K. Held. Adv. Phys. **56**, 829 (2007)

[153] K. Haule, J.H. Singh, G. Kotliar. Phys. Rev. Lett. **100**, 226402 (2008); arXiv: 0803.1279.

[154] A.O. Shorikov, M.A. Korotin, S.V. Streltsov, D.M. Korotin, V.I. Anisimov, S.L. Skornyakov, arXiv: 0804.3283.

[155] F. Aryasetiawan, M. Imada, A. Georges, G. Kotliar, S. Biermann, A.I. Lichtenstein. Phys. Rev. B **70**, 195104 (2004)

[156] T. Miyake, F. Aryasetiawan. Phys. Rev. B **77**, 085122 (2008)

[157] V.I. Anisimov, Dm. M. Korotin, S.V. Streltsov, A.V. Kozhevnikov, J. Kuneŝ, A.O. Shorikov, M.A. Korotin, arXiv: 0807.0547

[158] T. Miyake, L. Pourovskii, V. Vildosola, S. Biermann, A. Georges, arXiv: 0808.2442

[159] V.I. Anisimov, Dm. M. Korotin, M.A. Korotin, A.V. Kozhevnikov, J. Kuneŝ, A.O. Shorikov, S.L. Skornyakov, S.V. Streltsov, arXiv: 0810.2629

[160] V.I. Anisimov, O. Gunnarson. Phys. Rev. B **43**, 7570 (1991)

[161] E.Z. Kurmaev, R. Wilks, A. Moewes, N.A. Skorikov, Yu. A. Izyumov, L.D. Finkelshtein, R.H. Li, X.H. Chen, arXiv: 0805.0668

[162] T. Yildrim. Phys. Rev. Lett. **101**, 057010 (2008); arXiv: 0804.2252

[163] I.I. Mazin, M.D. Johannes, L. Boeri, K. Koepernik, D.J. Singh. Phys. Rev. B **78**, 085104 (2008); arXiv: 0806.1869.

[164] I.I. Mazin, M.D. Johannes. Nature Physics (in press); arXiv: 0807.3737

[165] V.A. Moskalenko, M.E. Palistarnt, V.M. Vakalyuk. Usp. Fiz. Nauk (Physics Uspekhi) **161**, 155 (1991)

[166] V. Barzykin, L.P. Gor'kov. Pis'ma v ZhETF (JETP Letters) **88**, 142 (2008); arXiv: 0806.1993

[167] L.V. Keldysh, Yu.V. Kopaev. Fiz. Tverd. Tela (Sov. Phys. Solid State) **6**, 2791 (1964)

[168] A.N. Kozlov, L.A. Maksimov. Zh. Eksp. Teor. Fiz. (JETP) **49**, 1284 (1965)

[169] B.I. Halperin, T.M. Rice. Solid State Physics. Ed. by F. Seitz, D. Turnball, H. Ehrenreich. Vol. 21, Academic Press, NY, 1968, p. 115

[170] Yu.V. Kopaev. Proc. P.N. Lebedev Phys. Institute **86**, 3 (1975)

[171] B.A. Volkov. Proc. P.N. Lebedev Phys. Institute **104**, 3 (1978)

[172] G.E. Volovik, L.P. Gor'kov. Pis'ma v ZhETF (JETP Letters) **39**, 550 (1984)

[173] G.E. Volovik, L.P. Gor'kov. Zh. Eksp. Teor. Fiz. (JETP) **88**, 1412 (1985)

[174] D. Parker, O.V. Dolgov, M.M. Korshunov, A.A. Golubov, I.I. Mazin, arXiv: 0807.3729

[175] P.B. Allen, R.C. Dynes. Phys. Rev. B **12**, 905 (1975)

[176] H. Eschrig, arXiv: 0804.0186

[177] D. Bhoi, P. Mandal, arXiv: 0808.2695

[178] R.H. Liu, T. Wu, G. Wu, H. Chen, X.F. Wang, Y.L. Xie, J.J. Yin, Y.J. Yan, Q.J. Li, B.C. Shi, W.S. Chu, Z.Y. Wu, X.H. Chen, arXiv: 0810.2694

[179] P.B. Allen, W.E. Pickett, H. Krakauer. Phys. Rev. B **37**, 7482 (1988)

[180] X.-L.Qi, S. Raghu, C.-X. Liu, D.J. Scalapino, S.-C. Zhang, arXiv: 0804.4332

[181] A.V. Chubukov, D. Efremov, I. Eremin, arXiv: 0807.3735

[182] Problem of High Temperature Superconductivity (Ed. by V.L. Ginzburg and D.A. Kirzhnits). "Nauka", Moscow 1977